ELECTROSTATIC PROCESSES

Static electricity is one of the earliest phenomena to be observed in physics. It aroused curiosity to understand the origin of the generation and movement of electrostatic charges. Contact electrification, or *triboelectric charging,* was discovered as early as 600 B.C. The investigation of static charges is the origin of our study of electricity: William Gilbert in the sixteenth century coined the term "electrical" from the Greek word for amber because amber and other resinous material charge so easily. During the seventeenth and most of the eighteenth century, the understanding of static electricity was primarily qualitative. However, a fundamental advance in our understanding of atmospheric static electricity was made by Benjamin Franklin. In the nineteenth century the pioneer studies on static electricity by scientists like Coulomb, Faraday, Maxwell, and Gauss laid the foundation of electrostatics. In the twentieth century, *current,* or flowing electricity, became an indispensable part of our daily lives in residential and industrial applications, from household appliances to transportation, from consumer electronics to supercomputers. However, the application of static electricity was not fully realized until late in the twentieth century. By then industrial electrostatic precipitators were widely used for gas cleaning and the electrophotographic process in copy machines and laser printers, which has become a billion dollar industry worldwide. Other major uses of static electricity include ink-jet printing, powder paint coating, electrostatic separation of impurities from minerals, and biomedical and pharmaceutical applications.

Along with the phenomenal growth of the semiconductor industry came concerns about the abatement of electrostatic discharge (ESD) in the development of circuit chips. During the last 50 years, a major effort has been focused on eliminating electrostatic charges, which are often a nuisance and in many cases extremely hazardous. A static discharge in many products may trigger explosions involving particulate materials. Electrical discharges can damage electronic circuitry, cause unwanted exposure of photographic films, and cause explosions during transfer of materials. Safety techniques and equipment have been developed for neutralizing static charge and to minimize industrial hazards. Several organic and inorganic materials are used as antistatic agents in carpet coatings and clothes drying.

Electrostatic processes are distinguished from electromagnetic processes in that electrostatic charges are stored in different media and the movement of the charges is either a discontinuous or a slow process. The associated magnetic fields are often negligible and are not considered.

To understand the electrostatic process, the fundamental concepts are discussed first. These concepts are related to

electrostatic charge, the coulombic forces of attraction and repulsion, the role of the dielectric constant of the medium in which charges are placed, the electric field and its relationship to the electric potential, Gauss's law, and Poisson's and Laplace's equations. These concepts are reviewed briefly in the following section. Most electrostatic processes involve charging and discharging. In order to explain the application of electrostatic processes, these mechanisms are discussed in the next two sections to provide an overview of the following topics: (1) charging of materials, (2) electrostatic atomization, (3) transport of charged particles, (4) deposition of charged particles, (5) separation of charged particles, (6) charge decay, (7) adhesion of charged particles, (8) electrostatic charges and electrostatic hazards, and (9) electrostatic charge neutralization. Applications are discussed in the subsequent sections: electrostatic precipitators, ink-jet printing, powder coating, electrophotography (copying machines and laser printers), electrostatic separation, and electrostatic hazard control. Additional books that provide excellent descriptions of these and other electrostatic processes are listed in the Reading List.

FUNDAMENTAL CONCEPTS OF ELECTROSTATIC PROCESSES

Electronic Charge

The electrostatic charge q_e of a single electron is

$$q_e = -1.602 \times 10^{-19}\ \text{C} \tag{1}$$

where C stands for the unit of charge named after Coulomb. The charge on the electron is the smallest fundamental charge in electrostatics.

Coulomb's Law

Coulomb's law describes the quantitative relationship of the electrostatic forces between charged bodies. The force between like charges is repulsive, and that between opposite charges is attractive. The force acts along a line between charge centers as shown in Fig. 1, and has a magnitude given by

$$F_C = \frac{q_1 q_2}{4\pi\epsilon_0 r^2} \tag{2}$$

where F_C is the coulombic force in newtons (N), q_1 and q_2 are two charges separated by a distance r, and ϵ_0 is the permittivity of free space, given by

$$\epsilon_0 = 8.854 \times 10^{-12}\ \text{F/m} \tag{3}$$

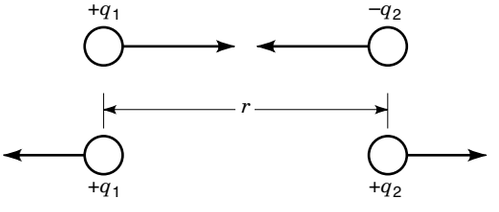

Figure 1. Coulombic forces of attraction and repulsion between two charges q_1 and q_2.

Table 1. Dielectric Constants of Some Common Materials

Medium	Dielectric Constant
Free space (vacuum)	1.0
Air, most gases	≈1.0
Insulating oil	2.2
Plastics (polystyrene, nylon, Plexiglas, Teflon, etc.)	2.1 to 3.5
Water	80
Aluminum oxide	8.80
Titanium dioxide (rutile)	173 (perpendicular)
	86 (parallel)
Barium titanate	1200

Equation (2) shows that the coulombic force obeys an inverse square law similar to that of gravitational and magnetic forces. The unit of permittivity is the farad per meter.

Dielectric Constant and Permittivity

If two charges are embedded in a dielectric medium , the coulombic force acting between them is reduced by the dimensionless dielectric constant of the medium, ϵ_r:

$$F = \frac{q_1 q_2}{4\pi\epsilon_0\epsilon_r r^2} \tag{4}$$

There is a decrease in the coulombic force and the electric field between the two charges because $\epsilon_r \geq 1$ for all materials:

$$F_e(\text{dielectric material}) = \frac{F_e(\text{vacuum})}{\epsilon_r} \tag{5}$$

For example, pure water has a dielectric constant of 80; this means the electrostatic force between the charges is reduced by a factor of 80. Most gases, including air, have a dielectric constant very close to one; most insulating solids have a dielectric constant in the range of 2 to 3, with a few exceptions, as shown in Table 1.

No electric field exists in a conducting medium, whereas an electric field can exist inside a dielectric medium. In conductors, charges are free to move until the potential difference between two points in the medium becomes zero. In a perfect insulator there is no flow of charges. The electric field across the insulating medium polarizes the atoms and molecules. Positive and negative ions are displaced in the dielectric medium; induced or permanent dipoles in atoms or molecules in the material line up partially according to their polarizability as the charges are displaced by the electric field. There is an induced charge on the surface as shown in Fig. 2. This induced charge appears on the surface across the medium when the electric field is applied. The induced charge per unit area is called the *displacement* $\boldsymbol{D}$. Both electric field $\boldsymbol{E}$ and displacement field $\boldsymbol{D}$ are vectors related by the permittivity of free space and the dielectric constant of the medium ($\epsilon_0\epsilon_r$):

$$\boldsymbol{D} = \epsilon_0\epsilon_r\boldsymbol{E} \tag{6}$$

The unit of $\boldsymbol{D}$ is in coulombs per square meter, whereas the unit of $\boldsymbol{E}$ is in volts per meter.

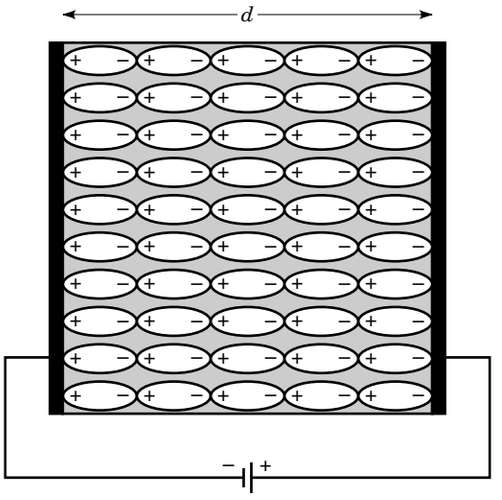

Figure 2. A thin layer of induced surface charge forms when a dielectric medium, placed in an electric field, polarizes.

Electric Field

The coulombic force experienced by a charge q_1 due to a second charge q_2 separated by a distance r in a dielectric medium can be written as

$$F = q_1 E \tag{7}$$

where E is the electric field due to the presence of charge q_2. Therefore, the electric field E at a distance r due to a charge q_2 is

$$E = \frac{q_2}{4\pi\epsilon_0\epsilon_r r^2} \tag{8}$$

Equation (7) can be expressed in the vector form

$$\boldsymbol{F} = q\boldsymbol{E} \tag{9}$$

where $\boldsymbol{F}$ is the coulombic force and $\boldsymbol{E}$ is the applied electric field.

When there are more than two charges involved, the force and the field are expressed as vector sum of the contributions from all other charges:

$$\boldsymbol{F} = \boldsymbol{F}_{12} + \boldsymbol{F}_{13} + \boldsymbol{F}_{14} + \boldsymbol{F}_{ij} \tag{10}$$

$$\boldsymbol{E} = \boldsymbol{E}_{12} + \boldsymbol{E}_{13} + \boldsymbol{E}_{14} + \boldsymbol{E}_{ij} \tag{11}$$

where $\boldsymbol{F}_{ij}$ and $\boldsymbol{E}_{ij}$ represent the force and field, respectively, between charges q_i and q_j.

Electric Potential or Voltage

The *electric potential* at a point is defined as the work done in moving a unit charge from infinity (where the potential is zero) to the point in question. Since work is defined as force times distance, the potential V can be written as

$$\begin{aligned} V &= \int \boldsymbol{E} \cdot d\boldsymbol{r} \\ &= -\int q\boldsymbol{E} \cdot d\boldsymbol{r} \end{aligned} \tag{12}$$

The negative sign arises because work is done on the unit charge ($q = 1$) to move it against the field $\boldsymbol{E}$ to the point in question. If the point is designated as A, then

$$V_A = -\int_{\infty}^{A} q\boldsymbol{E} \cdot d\boldsymbol{r} \tag{13}$$

The potential difference V_{AB} between two points A and B can be written as

$$V_{AB} = -\int_{A}^{B} q\boldsymbol{E} \cdot d\boldsymbol{r} \tag{14}$$

The potential V is a scalar quantity and not a vector like $\boldsymbol{E}$ and $d\boldsymbol{r}$. Clearly, the electric field $\boldsymbol{E}$ is obtained from the voltage gradient, given by

$$\boldsymbol{E} = -\frac{dV}{d\boldsymbol{r}} = -\text{grad}\, V \tag{15}$$

Using del, we can write

$$\boldsymbol{E} = -\nabla V \tag{16}$$

The relationship between the potential V and the electric field $\boldsymbol{E}$ can be illustrated in a parallel plate capacitor as shown in Fig. 3. A capacitor is formed by two parallel conducting plates, A and B, separated by a distance d. The potential across the plates is given by

$$V_{AB} = -\int_{A}^{B} \boldsymbol{E} \cdot d\boldsymbol{r} = Ed$$

where

$$E = -\frac{V_{AB}}{d} \tag{17}$$

Figure 3 shows that the potential is constant everywhere on the surface of a conducting plate. The electric field is constant throughout the homogenous medium between the plates, neglecting the boundaries.

Electric Field Lines and Equipotential Surfaces

A conducting electrode is an equipotential surface in space. The conducting surface has a large number of charges free to rearrange themselves so as to maintain a constant potential across the surface. A *Faraday cage* is a conductive surface surrounding an object and held at a known potential. In some

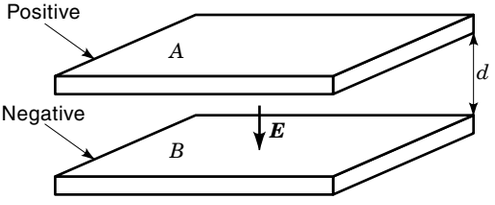

Figure 3. The potential difference and electric field across a parallel plate capacitor.

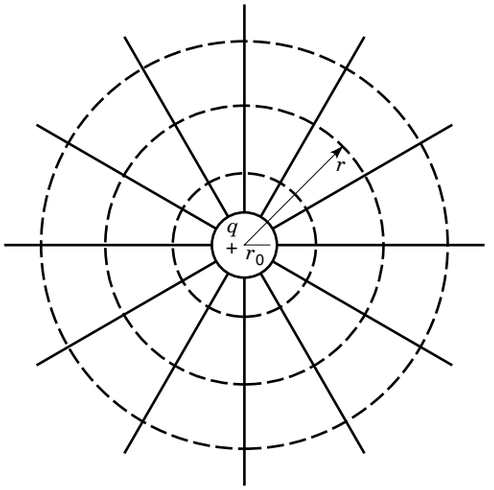

Figure 4. Field lines and equipotential surfaces related to an isolated conducting sphere of radius r_0. The solid lines represent field lines, and the broken curves represent equipotential surfaces. Since q is positive, the field lines are directed radially outward.

applications, the cage is a grounded screen (potential zero) and surrounds sensitive electronic equipment to protect it from being damaged by external electrostatic fields. A Faraday cage is often used for shielding electrostatic measurements.

Electric field lines and equipotential surfaces can aid our visualization of electrostatic forces and movement of charged particles. Depending upon the geometry and location of electrodes, the field lines and equipotential surfaces can be mapped according to the following criteria:

1. $\boldsymbol{E} = -\text{grad}\ V = -\boldsymbol{\nabla} V$.
2. There can be no potential difference along a surface of a conductor.
3. Any point in space can have only one potential at any given instant of time.
4. Equipotential surfaces cannot intersect.
5. Field lines are always perpendicular to equipotential surfaces.

The imaginary field lines and equipotential surfaces related to an isolated conducting sphere having a charge q are shown in Fig. 4. Since all the points on the surface of the conducting sphere are at the same potential, an equipotential surface close to the conducting surface must be parallel to it. The equipotential surfaces are shown as broken curves. The field lines (shown as solid lines) are perpendicular to the equipotential surfaces, and so are directed radially outward from the positive conducting sphere. These lines represent the direction of the electric field.

Field lines always originate on charges and end on opposite charges. The density of the field lines represents the magnitude of the electric field (E) caused by the charge.

Gauss's Law

Let us consider the equipotential spherical surface of radius r as shown in Fig. 4. The field E at any point on the surface is given by Coulomb's law [Eq. (8)]:

$$E = \frac{q}{4\pi\epsilon_0 r^2} \tag{18}$$

The surface area S of the spherical shell of radius r is

$$S = 4\pi r^2 \tag{19}$$

The product of these two quantities is

$$ES = \frac{q}{\epsilon_0} \tag{20}$$

If the charge is inside a dielectric medium, then Eq. (20) is written in the form

$$ES = \frac{q}{\epsilon_0 \epsilon_r} \tag{21}$$

or

$$\epsilon_0 \epsilon_r = ES = q \tag{22}$$

This relationship holds true for any closed surface S of any shape that encloses one or more charges. This is *Gauss's Law,* which can be written in the form

$$\int_S (\epsilon_0 \epsilon_r \boldsymbol{E}) \cdot d\boldsymbol{S} = \sum q \tag{23a}$$

From Eq. (6), $\epsilon_0 \epsilon_r \boldsymbol{E} = \boldsymbol{D}$; therefore

$$\int_S \boldsymbol{D} \cdot d\boldsymbol{S} = \sum q \tag{23b}$$

where Σq represents the sum of all charges enclosed by the surface of area S. Since $\boldsymbol{D}$ represents induced charge per unit area, Gauss's law states that for a closed surface S of any shape, the surface integral of the induced charge per unit area over S gives the sum of all charges enclosed by S. The electric field and the displacement can vary over the surface S, but the integral of the product is the sum of all charges enclosed. Gauss's law can be used to calculate the field due to several charges distributed in space or to calculate the total charge from the measured electric field.

For example, if the charges are distributed uniformly, then within a volume V enclosed by a surface S,

$$\int_S \boldsymbol{D} \cdot d\boldsymbol{S} = \sum q = \int_V q_v \, dV \tag{24}$$

where q_v is the total net charge per unit volume enclosed by the surface S. Since $\int_S \boldsymbol{D} \cdot d\boldsymbol{S}/dV$ is the flux per unit volume, or the divergence, the divergence form of the above equation can be written as

$$\nabla \cdot \boldsymbol{D} = q_v \tag{25}$$

or

$$\nabla \cdot \boldsymbol{E} = q_v \epsilon_0 \epsilon_r \tag{26}$$

Poisson's and Laplace's Equations

Equation (16) showed the relationship between the electric potential V and the field $\boldsymbol{E}$. In most cases, both V and $\boldsymbol{E}$ are functions of location ($\boldsymbol{r}$); therefore, a general form of the same equation can be written as

$$\boldsymbol{E}(\boldsymbol{r}) = -\nabla V(\boldsymbol{r})$$

We often need to estimate $V(\boldsymbol{r})$ from the distribution of charge q_v. If we combine Gauss's law with the field–potential relationship, we can substitute Eq. (16) in Eq. (26):

$$\nabla \cdot \boldsymbol{E} = q_v/\epsilon_0\epsilon_r$$
$$\nabla \cdot (\nabla V) = -q_v/\epsilon_0\epsilon_r$$

or

$$\nabla^2 V = -q_v/\epsilon_0\epsilon_r \tag{27}$$

Equation (27) is known as Poisson's equation. It can be used to calculate the potential distribution from the volume density of charge. When q_v is known, this equation can be used to calculate $V(\boldsymbol{r})$. We have assumed ϵ_r is independent of the spatial coordinates.

In the regions where the net charge density is zero ($q_v = 0$) Poisson's equation becomes *Laplace's equation:*

$$\nabla^2 V = 0 \tag{28}$$

Most electrostatic processes can be analyzed using the relationships above. Therefore, it is desirable to understand the physical concepts underlying Coulomb's law, Gauss's law, Poisson's equation, and Laplace's equation. To describe many electrostatic processes, the distribution of the electric field is often needed for a given electrode geometry. Once these boundary conditions and a knowledge of the volume charge distribution are specified, analytical and numerical techniques are available to solve Laplace's and Poisson's equations.

Capacitance

A capacitor has the ability to store electrostatic charge. In an isolated conductor of charge q as shown in Fig. 4, the ratio of its charge Q and potential V is defined as the capacitance C:

$$C = Q/V \tag{29}$$

Where Q is expressed in coulombs (C) and V in volts (V), C will be in farads (F).

In the parallel plate capacitor of Fig. 3, the electric field is given by Eq. (17). The total charge Q on each plate is determined using Gauss's law [Eq. (23a)]:

$$\int_S (\epsilon_0\epsilon_r \boldsymbol{E}) \cdot d\boldsymbol{S} = \sum q = Q$$

Table 2. Volume Resistivity of Different Materials

Material	Volume Resistivity ($\Omega \cdot$ m)
Polystyrene, PTFE	10^{17} to 10^{18}
Glass, nylon	10^{10} to 10^{12}
Oils	10^{9}
Distilled water	10^{6}
Sea water	1
Metals	10^{-7}

Since $E = V/d$,

$$\epsilon_0\epsilon_r \frac{V}{d} A = Q$$

where A is the surface area of each plate. Since

$$C = Q/V = \epsilon_0\epsilon_r A/d \tag{30}$$

the energy U stored in the capacitor is

$$U = \tfrac{1}{2}CV^2 = \frac{1}{2}\frac{Q^2}{C} \tag{31}$$

Resistivity

Electrical resistivity plays a very important role in many electrostatic processes, particularly in charge decay. The electrical resistivity of a material, ρ, is related to the resistance R by

$$\rho = RA/l \qquad (\Omega \cdot \text{m}) \tag{32}$$

where A is the cross-sectional area, l is the length of the material, and R is the resistance in ohms.

There are two components of resistivity: (1) volume resistivity ρ_v as defined above, and (2) surface resistivity ρ_s. Both are important, since charge can leak over the surface or through the material. The volume resistivity is expressed in ohm-meters. The surface resistivity is expressed in ohms per square ($\Omega/\square$).

The volume resistivity varies widely for different materials, as shown in Table 2.

Charge Decay

In a typical insulator, charge does not leak off quickly as in a conductor, but decays at a low rate depending upon the resistivity of the materials and, in the case of a nonlinear resistive material like polymer powder, the potential across it. The decay of charge q_0 across the dielectric medium of a capacitor can be described by the simple exponential expression

$$q = q_0 \exp(-t/\tau) \tag{33}$$

where τ is the charge decay relaxation time constant defined as the product of the dielectric constant ϵ_r of the material, its resistivity ρ, and the permittivity of free space, ϵ_0:

$$\tau = \epsilon_0\epsilon_r\rho \tag{34}$$

The charge decay relaxation time is a lumped parameter and can easily be measured experimentally. If the dielectric constant is known or can be measured, the resistivity can be determined using Eq. (34).

The measured resistance of an insulator may be largely due to absorbed moisture or contaminants on its surface rather than to its intrinsic volume resistivity. Great care should be taken when measuring volume resistivity to avoid surface contamination.

Flow of Charge and Current

In electrostatic processes, the current is defined by the rate of flow of charge:

$$i = \frac{dq}{dt} \qquad \text{(A)} \tag{35}$$

It is carried by ions, electrons, and charged particles. Thus the total current i_t is given by

$$i_t = i_i + i_p + i_e \tag{36}$$

For example, in a typical electrostatic powder spray process, powder particles are charged by ions. The total current is due to electron current, ion current, and charged particle current. In powder coating applications employing corona guns, the total current is primarily ion current. Corona charging is discussed in the next section.

When current is distributed over a surface, the concept of surface current density J (A/m^2) is important. It is related to current by

$$i = -\oiint \boldsymbol{J} \cdot d\boldsymbol{A} \qquad \text{(A)} \tag{37}$$

where the negative sign indicates that current is considered positive when dq/dt is positive; that is, the flow of current increases the charge [Eq. (35)]. The total current density is given by summing the current densities of the charge carriers:

$$\boldsymbol{J} = \sum \boldsymbol{J}_i = \sum n_i q_i \mu_i \boldsymbol{E} \equiv \sigma \boldsymbol{E} \tag{38}$$

where n_i, q_i, and μ_i are the number density, magnitude of charge, and mobility of each carrier type i, respectively, and $\boldsymbol{E}$ is the applied electric field. The conductivity σ of a medium is defined by the summation of the products $n_i q_i \mu_i$.

Electrostatic Breakdown Field

From Gauss's law the electric field at the surface of an imaginary sphere that contains a total charge q is given by Eq. (22):

$$ES = \frac{q}{\epsilon_0 \epsilon_r}$$

Thus we can write

$$E = \frac{q}{S} \cdot \frac{1}{\epsilon_0 \epsilon_r} = \frac{Q_s}{\epsilon_0 \epsilon} \tag{39}$$

where Q_s is the surface charge density in coulombs per square meter. In air, when E exceeds the breakdown voltage E_b, which is nearly equal to 3.0×10^6 V/m, the surface charge will dissipate through air ionization. Therefore, the maximum surface charge density in air ($\epsilon_r = 1$) is

$$\begin{aligned} Q_s(\max) &= \epsilon_0 E_b \\ Q_s(\max) &= 3.0 \times 10^6 \times 8.854 \times 10^{-12}\ \text{C/m}^2) \\ &= 2.65 \times 10^{-5}\ \text{C/m}^2 \end{aligned} \tag{40}$$

In general, the maximum electric field is determined by the medium that surrounds the surface. In free space (vacuum), the electric field can be increased until field emission of electrons or ions from the surface occurs.

When the electric field between two electrodes in air exceeds the breakdown voltage, the air ionizes, causing ion current. Depending on the electrode geometry and the voltage applied to the electrodes, there will be either a sustained corona or a spark. An overview of corona and sparking processes is given later, but the energy involved in an electrostatic sparking process is illustrated below.

Energy of Electrostatic Sparks

If an isolated charged conductive sphere of capacitance C, whose surface potential is V, discharges in air by means of a spark, then it dissipates more than 90% of its total energy

$$U = \tfrac{1}{2} CV^2 \tag{41}$$

A spark is generally characterized by the production of a high concentration of ions (10^{16} ions/m^3) in a short period of time (1 μs). This discharged energy is one of three important criteria for predicting an explosion in a medium that may contain flammable vapor or particulate materials. The other two criteria are the concentration of the combustible materials and the concentration of oxidizing agents, such as oxygen in air. For organic solvents, the minimum ignition energy is about 0.3 mJ. Electrostatic hazard control is discussed below in the section so named. One primary difference between spark and corona discharge is that a spark is characterized by a negative resistance so that an unstable high current discharges in a very short time period, whereas a corona discharge is stable and has positive resistance.

CHARGING OF MATERIALS AND TRANSPORT OF CHARGED PARTICLES

Charging of Materials

The three most important mechanisms used in charging materials are: (1) corona charging, (2) induction charging, and (3) contact charging, or *tribocharging*. Materials can also be charged by nuclear or ultraviolet (UV) radiation, which ejects electrons from the surface, leaving a net charge on it. In this section, we will discuss in detail the three main mechanisms of charging as well as the transport, deposition, and separation of the charged particles according to the applications.

Corona Discharge

Let us consider two electrodes (Fig. 5), one of which is a wire and has a small radius of curvature, placed coaxially inside a cylindrical pipe. The wire is held at a high potential, and the cylinder is grounded. The electric field near the small-radius wire electrode will have a high intensity. Free electrons in this high-intensity field region will be accelerated and move away from the negative central wire toward the grounded cylinder at high velocities because of their high electrical mobility.

When the energy of these electrons is sufficiently high to produce electron–ion pairs upon impact with neutral gas molecules, ionization occurs. This ionization process repeats many times, creating an avalanche of electrons and positive ions in the high-electric-field region called the corona glow. The process is similar for both positive and negative corona discharges except that the directions of motion of ions and electrons are reversed.

The bluish light emitted in this region because of the high-energy electron collision with the molecules is called a corona. The word comes from the Latin word for "crown" and was coined by sailors who observed corona glow around the masts of their ships during thunderstorms. Most of the radiation is in the blue and near-UV spectrum.

The avalanche process, shown in Fig. 6 for a point-to-plane geometry, is governed by the ionizing potential of gases present near the small-radius electrode. Some of the requirements of sustaining the corona process are (1,2):

1. The electron energy in electron volts (eV) must be greater than the ionization potential of the surrounding gas. For example, ionization potential for the O_2 molecule is 12.2 eV. The electron energy must exceed this value to ionize neutral O_2 molecules to O_2^+ ions and electrons. An electron volt is 1.6×10^{-19} C $\times$ 1 V = 1.6×10^{-19} J.

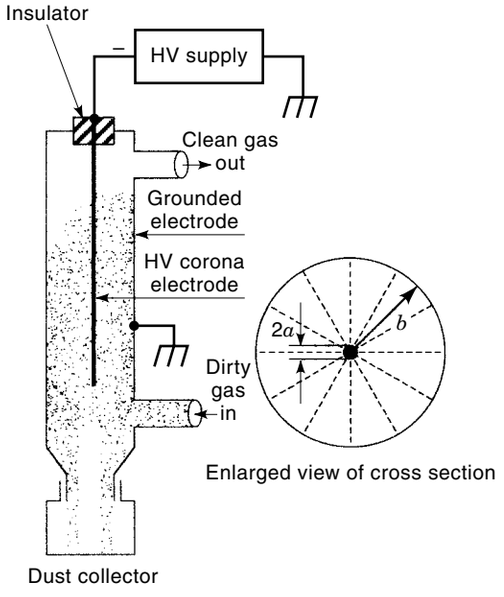

Figure 5. A wire–cylinder geometry of an electrostatic precipitator.

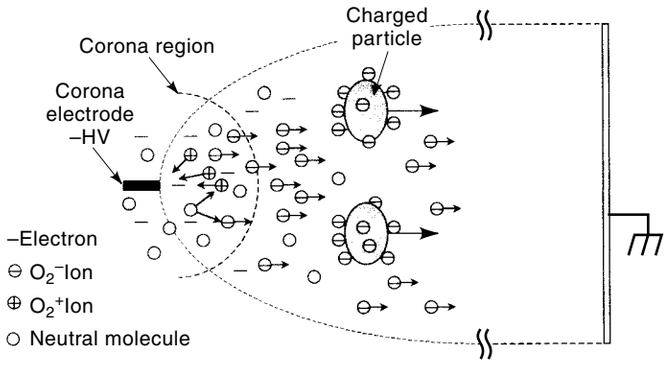

Figure 6. A point-to-plane electrode geometry showing negative corona breakdown of gas. In the corona region, free electrons accelerate to an energy sufficient to ionize neutral gas molecules. The process is repeated many times, causing an avalanche. As the stream of electrons moves toward the grounded electrode, there are electron attachments to form O_2^- ions. The negative ions then move toward the grounded electrode along the field lines and collide with particles. Both negative ions and the charged (negative) particles deposit on the grounded electrode.

2. Since not every collision between the moving free electrons and gas molecules will produce ionization, the ionization cross section or collision probability factor needs to be high to sustain a corona.
3. The corona discharge requires a source of *initiating electrons*. Under laboratory conditions, these are produced by cosmic rays, and have an average concentration of about 20 ion–electron pairs per cubic centimeter of air.
4. The electric field near the small-diameter electrode must be higher than the corona-initiating field. For a wire-cylinder geometry, Peek's equation (2) gives the minimum electric field required for ionization of air:

$$E_c = 3 \times 10^6 f(\delta + 3.0\sqrt{\delta/a}) \text{V/m} \tag{42}$$

where

f = roughness factor of the wire electrode (dimensionless)
δ = relative air density = $(T_0/T)(P/P_0)$
a = radius of the corona wire (m)
E_c = corona-initiating field (V/m)
T_0 = 298 K
T = actual temperature (K)
P_0 = 1 atm
P = actual pressure (atm)

The voltage V_c required to initiate corona in a wire cylinder geometry can be written as

$$V_c = 3 \times 10^6 af\left(\delta + 3.0\sqrt{\frac{\delta}{a}}\right)\ln\frac{b}{a}\text{V} \tag{43}$$

where a is the radius of the HV wire electrode, and b is the radius of the cylindrical electrode.

The above equation shows that V_c required to initiate corona increases with the wire radius a. As a decreases, there is a corresponding increase of the electric field near the wire.

Therefore, it is possible to initiate corona at a low voltage provided a is small and b/a is also small. For example, in a Corotron, a corona discharge device is used to charge the photoconducting drum surface, the voltage required to initiate and sustain corona is about 10 kV. In a powder coating booth, a voltage of -80 kV to -100 kV is applied to the powder coating gun to sustain corona current.

In powder coating or electrostatic precipitator applications, it is necessary to have a strong electric field near the collecting electrodes for efficient deposition of charged particles. The magnitude of the electric field near the collecting electrode decreases sharply as distance increases between the two electrodes and as the diameter of the corona wire electrode decreases. The volume of the corona region also decreases. Below a certain limit in the corona region, no avalanche can take place. The electric field in a wire–cylinder geometry, in the absence of free charges, can be written by solving Laplace's equation. Since b and a are both constants for a given electrode geometry (2), then

$$E(r) = \frac{V}{\ln(b/a)r} \tag{44}$$

The field is axisymmetrical and is inversely proportional to the distance r from the wire surface when there are no ions present. The effect of corona ions is to increase the field near the cylinder electrode and decrease it near the high-voltage electrode. However, for a reasonably high space charge, the electric field at a sufficiently large distance r from the wire can be approximated by (3)

$$E = \left(\frac{J}{2\pi\epsilon_0 b}\right)^{1/2} \qquad r \gg a \tag{45}$$

where J is the corona current per unit length of the wire. This approximate value of E is independent of r. Similarly, in a point-to-plane geometry, the field E is approximated by a value between V/d and $2V/d$, where d is the distance between the plane and the point electrode as shown in Fig. 6.

For a large high-voltage-electrode diameter, the field decreases less sharply with increasing distance from the discharge wire. Therefore, to increase the field near the grounded electrode, the diameter of the electrode should be as large as possible, consistent with corona generation. At very large values of a, the second term of the Eq. (42) can be neglected, so the corona field E_b for air is

$$E_b = 3 \times 10^6 \text{ V/m} \qquad \text{at NTP} \tag{46}$$

This is the air breakdown field E_b at normal temperature and pressure (NTP). Note that in vacuum there can be no corona discharge. The field can be increased, often by two orders of magnitude (to 10^8 V/m), when field emission of electrons or ions from the high voltage electrode surface sets the limit.

Electron Attachment by Gas Molecules

When a corona initiates, the total space charge density, ρ_t has three components:

$$\rho_t = \rho_e + \rho_i + \rho_p \tag{47}$$

Table 3. Electron Attachment Probabilities for Different Gases

Gas	Average No. of Collisions for Attachment
Inert gas	∞
N_2, H_2	∞
O_2	4×10^3
H_2O	4×10^4

where ρ is the space charge density, and the subscripts e, i, and p represent space charge components contributed by electrons, ions, and particles, respectively. If there are no electronegative gas ions present, then the space charge will be due to electron and charged particles, so that

$$\rho_t = \rho_e + \rho_p \tag{48}$$

Since electrons have high mobility, the current will be high and sparkover may occur. A sustained negative corona requires the presence of such electronegative gases as oxygen to produce negative ions.

Collision between electrons and electronegative molecules results in negative ions. The number of collisions needed for electron attachment depends on the type of gas, as shown in Table 3. For practical purposes, only a small amount of O_2, H_2O, or SO_2 is needed for electron attachment. These electronegative gases provide stable corona currents.

The corona current can be expressed as

$$J = (\rho_e b_e + \rho_i b_i + \rho_p b_p)E \qquad \text{(A)} \tag{49}$$

where the b's represent the mobilities of electrons, ions, and particles, respectively. In most applications of negative corona, the corona current is primarily conducted by negative ions. Because of the lower mobility of particles, $\rho_p b_p$ is negligible compared to $\rho_e b_e$ and $\rho_i b_i$. The electron current is small, since most of the electrons get attached to O_2 molecules. Thus

$$J = (\rho_e b_e + \rho_i b_i)E \qquad \text{(A)} \tag{50}$$

But the space charge due to the particles is significant; therefore

$$\rho_t = \rho_i + \rho_p \tag{51}$$

since each charged particle contains large numbers of unit charges.

Ion Wind

As the ions move in the drift region toward the grounded electrode, they collide with and impart energy to the neutral gas molecules, but without sufficient energy to cause ionization. However, the momentum transfer to air molecules results in an *ion wind* of typically 1 m/s to 2 m/s velocity.

Generally, corona initiation begins with a rapid current jump from nearly zero to a few microamperes. The current then rises with increasing voltage; in accordance the approximate relationship can be written as

$$I = KV(V - V_c) \tag{52a}$$

where K is a constant depending upon the geometries involved in the corona process, V is the applied voltage, and V_c is the corona-initiating voltage. For a point-to-plane geometry, the current density J (A/m^2) at the surface can be written as

$$J = KV(V - V_c)/d^2 \tag{52b}$$

where d is the perpendicular distance between the point and the plane electrode. The current density changes as the distance between the point electrode and target surface varies. J also varies with time as particles are deposited on the target and the particle cloud density changes in the interelectrode space.

Corona Charging of Substrates and Particles

Substrate Charging. Ions from a corona discharge can be used to charge particles or surfaces. For example, the photoconducting surface of an optical photoconductor (OPC) in a copying machine is charged by corona discharge. For an insulating surface, the ions deposit on the surface following the field lines. The maximum charge density is limited by the ionization of the air surrounding the surface. In air, the breakdown field intensity E_b cannot exceed 3×10^6 V/m. The maximum surface charge density Q_s at the breakdown point is obtained from

$$E_b = \frac{Q_s}{\epsilon_0} \tag{53}$$

For an isolated large flat surface with charge density Q_s, the field lines are perpendicular to the surface with magnitude $E = Q_s/\epsilon_0$ independent of the distance from the surface:

$$\begin{aligned} Q_s(\max) &= E_b\epsilon_0 \\ &= 2.64 \times 10^{-5}\ \text{C/m}^2 \end{aligned} \tag{54}$$

For a parallel plate capacitor of dielectric constant ϵ_r and thickness t, there will be a breakdown voltage setting the maximum surface charge limit of capacitors:

$$\begin{aligned} Q_s &= CV_s \\ V_s &= \frac{Q_s t}{\epsilon_0\epsilon_r} \end{aligned} \tag{55}$$

where t is the thickness of the insulating layer between the two conducting plates and Q_s is the surface charge density. For a dielectric film or a powder layer on a conducting plate, the surface voltage is thus limited by t and ϵ_r. In typical applications related to copying machines or laser printers, the surface voltage is of the order of 600 V for $t = 20$ μm and $\epsilon_r = 3$.

When charges accumulate on an insulating layer backed by a grounded metal plate, image charges develop across the dielectric film, forming a capacitor. Under such conditions, the field E external to the charged layer is almost zero, since the entire field becomes bound between the charged surface layer and its image charges across the dielectric film. A portion of the accumulated charge may leak through the film. This leakage depends upon the resistivity of the film or powder layer. Examples are charged fly ash deposition in electrostatic precipitators, optical photoconductor operation in printers, and deposition of charged powder on a grounded conducting workpiece in a powder coating process. Here the thin insulating layer acts like a distributed capacitor. Depending on the film thickness, a considerable amount of charge density, often in excess of the limit set by Eq. (44), may be present and lead to back corona, dielectric breakdown, and propagating brush discharge, depending upon the values of Q_s, t, and the dielectric breakdown strength (4). Table 4 shows the breakdown field for different dielectric media.

Table 4. Comparison of Terminal Settling and Electrical Migration Velocities for Particles with Maximum Charge

Particle Diameter (μm)	Terminal Settling Velocity (cm/s)	Terminal Electrical Migration Velocity (cm/s)
0.2	0.0002	1
2	0.013	10
20	1.2	100
100	25	500
200	70.8	1000

Particle Charging. A particle placed in an electric field is polarized and therefore attracts ions of both polarities. In an electric field containing unipolar ions and uncharged particles, the particles will acquire charge of one polarity due to the local deformation of the electric field. Similarly, a charged particle can be neutralized in a biionized field. The electric field is distorted by the presence of the particles, and as the particles acquire charge, the distortion changes. The ions follow the electric field lines that terminate on the particle, and charging continues until the retained charge on the particle repels additional ions. Saturation charge occurs when the attractive field due to field distortion equals the repulsive field due to the charge on particles. This charging process is known as *field charging*. For a spherical particle of radius r in an electric field E, the maximum charge limit is known as the Pauthenier limit, first derived by Pauthenier (3):

$$Q_{\max} = 4\pi\epsilon_0 r^2 pE \tag{56}$$

where r is the particle radius, $p = 3\epsilon_r/(\epsilon_r + 2)$, ϵ_r is the dielectric constant, and E is the electric field. For a conducting particle one has $\epsilon_r = \infty$, $p = 3$, and for a highly insulating particle, $\epsilon_r = 1$, $p = 1$.

The charge-to-mass ratio of a spherical particle of density ρ_p can be calculated as follows:

$$\begin{aligned} m &= \tfrac{4}{3}\pi r^3\rho \\ \frac{q_{\max}}{m} &= \frac{4\pi\epsilon_0 r^2 pE}{\frac{4}{3}\pi r^3\rho_p} = \frac{3\epsilon_0 pE}{\rho_p r} = \frac{6\epsilon_0 p}{\rho_p d_p}E \end{aligned} \tag{57}$$

where d_p is the particle diameter, and $(q/m)_{\max}$ is the maximum charge-to-mass ratio in an electric field E in a corona charging process.

For a spherical particle, the maximum charge-to-mass ratio (1) varies linearly with E; (2) varies inversely with the particle diameter d_p, (3) is a weak function of ϵ_r, and (4) does not depend on the density of ions.

The density of ions influences the time it takes for a particle to reach its saturation charge. The charge on a particle at any time t is given by

$$q = q_{\max}\frac{1}{1+\tau/t} \tag{58}$$

where τ is the time taken by the particle to reach one-half the saturation charge and is given by

$$\tau = 4\epsilon_0/N_0 eb \tag{59}$$

where N_0 is the ion density (ions/m^3), b is the mobility of ions, and e is the electronic charge. The particle acquires 50% of its charge at $t = \tau$ and 95% of its saturation during the time period 3τ.

Electrical Mobility

The electrical mobility Z is the velocity of a charged particle in an electric field of unit strength and is related to the electrical migration velocity V_e of a particle in a field E by

$$V_e = ZE$$

or

$$Z = V_e/E \tag{60}$$

For a spherical particle of charge q and moving in a uniform electric field,

$$Z = q/3\pi\eta d_p \tag{61}$$

where η is the viscosity of the medium and d_p is the diameter of the particle.

Electrical Migration Velocity

The electrostatic force on charged particles free to move in a dielectric medium will soon attain a terminal electrostatic migration velocity when the driving force qE becomes equal to the drag resistance force. The electrostatic force on a particle of charge q in an electric field E can be written

$$F_e = qE \tag{62}$$

The drag force F_d on the particle, assuming Stokes's law is valid (particle motion at small Reynolds number $Re_p < 1$), can be written

$$F_d = 3\pi\eta d_p V_e \tag{63}$$

where V_e is the particle velocity relative to the medium. Assuming the particle is charged to the Pauthenier limit in an electric field E, the surface charge density is Q_s and is given by

$$Q_s = q/4\pi r^2$$

When $F_e = F_d$, we have the terminal electrical migration velocity

$$Q_s 4\pi r^2 E = 6\pi\eta r V_e$$

or

$$V_e = \frac{qE}{6\pi\eta r} = \frac{Q_s d_p E}{3\eta} \tag{64}$$

Equation (64) shows that when particles are charged to their saturation limit, the electrical migration velocity is directly proportional to the diameter of the particle and the electric field.

For example, if the electric field is 10^5 V/m, then the electrical migration velocity $V_e \approx 10$ m/s for a particle diameter $d_p = 200$ μm, $V_e \approx 1$ m/s for $d_p = 20$ μm, and $V_e \approx 10$ cm/s for $d_p = 2$ μm. We can compare these velocities with the gravitational settling velocities for particles of different sizes, since

$$F_g = mg = \tfrac{4}{3}\pi r^3 \rho_p g \tag{65}$$

The particles reach terminal settling velocity when $F_g = F_d$. The terminal settling velocity V_{TS} can be approximated (for $d_p < 100$ μm) as

$$V_{TS} \approx 0.003 d_p^2 \text{ cm/s} \tag{66}$$

where d_p is in micrometers. The examples in Table 4 show that V_e can be much larger than V_{TS}.

Clearly, the electrical migration velocity for particles up to a certain diameter (approximately 24 mm) charged to the Pauthenier limit is much larger than the gravitational settling velocity. The electrical migration velocity increases linearly with the diameter d, whereas the settling velocity increases with the square of the diameter (d^2). However, the electrical migration velocity for small particles is often negligible compared to the aerodynamic forces in a turbulent air flow field. For particles in the size range 1 μm to 1000 μm, the electrostatic forces can be made to dominate both gravitational and aerodynamic forces in applications related to electrostatic precipitators, electrostatically charged filters, powder coating, and charge separators.

Back Corona

Back corona is the ionization of powder deposited on a conducting substrate due to a high electric field across the powder layer. Back corona plays an important role in electrostatic precipitation and in powder coatings, and occurs when powder has high resistivity. Even a monolayer of highly resistive powder deposited on the conducting substrates can produce back corona. The continuous bombardment of the powder with ions can cause the field strength to exceed the breakdown field strength of air ($E_b = 3 \times 10^6$ V/m) a few seconds after deposition begins. The deposition rate on the surface of the workpiece rapidly decreases because of the back corona, causing the thickness buildup of the powder layer to slow down. Eventually a point is reached when the back corona prevents further deposition.

When back corona at the deposited, negatively charged powder layer occurs, positive ions start migrating toward the negative-corona gun electrode. This stream of positive ions will neutralize the oncoming negatively charged particles, adversely affecting the deposition process in the areas of back corona. Since back corona occurs randomly on the surface, it produces a random variation of film thickness. At each point of back corona initiation, there is an eruption of powder from

the surface because of the breakdown and polarity reversal of powder charging. Under severe back corona, the intensity is sufficiently strong to fuse the powder particles where the breakdown occurs. Back corona causes the powder film to appear "spot-welded" all over the surface, resulting in tiny craters, pinholes, and an orange-peel appearance after curing. In general, back corona limits the efficiency of the electrostatic deposition of powder and it alters the appearance of the film in a powder coating process.

In summary, back corona:

1. Occurs when high-resistivity fly ash or polymer powder deposits on a surface, causing the electric field across the powder layer to exceed the breakdown voltage of the dielectric medium surrounding the powder layer.
2. Creates ions of opposite polarity, which discharge the powder and disrupt the deposition process.
3. Rapidly decreases the efficiency of the powder deposition.
4. Results in overspray of powder within a few seconds.
5. Decreases the deposition rate in those areas where there is a sufficient powder buildup. However, the deposition rate remains high where there is no back ionization and the layer thickness is low. Thus, the buildup of the powder layer across the entire surface is a self-limiting process resulting in a fairly uniform thickness of powder film.
6. Causes pinholes, moon craters, and orange peels in the cured film.
7. Limits the electric field strength across the powder layer to approximately 5×10^6 V/m. Therefore, for a film thickness of 100 μm, the voltage drop will be given by

$$E_b = \frac{V_d}{d}$$
$$V_d = 5 \times 10^6 \times 100 \times 10^{-6}\,\text{V}$$
$$= 500\,\text{V}$$

Here

$$V_d = J\rho t \tag{67}$$

where J is the current density, ρ is the resistivity of the powder layer, and t is the film thickness; we have

$$J = E/\rho \qquad (\text{A/m}^2) \tag{68a}$$

For a powder resistivity of $10^{15}\ \Omega \cdot \text{m}$,

$$J = \frac{5 \times 10^6\ \text{V/m}}{10^{15}\ \Omega \cdot \text{m}} = 5 \times 10^{-9}\ \text{A/m}^2 \tag{68b}$$

This current density is much smaller than the forward corona density of 10^{-4} A/m^2 in an electrostatic precipitator. It signifies that ion currents higher than this value will lead to a condition where excess ions either are finding a path to ground or are being deposited on the powder layer, increasing the surface charge. This shows that the volume conduction of current through the powder is relatively small, meaning back corona is influenced more by the interstitial air and the powder surface condition.

If the workpiece surface has protuberances, the electrical field intensifies at those points and breakdown will occur there first. Therefore, surface irregularities, including sharp edges, strongly influence the occurrence of back corona.

Diffusion Charging

While field charging is the dominant charging mechanism for particles larger than 2 μm in diameter, diffusion charging becomes important for particles smaller than 1 μm in diameter. It is independent of the electric field E. Diffusion charging arises from the thermal motion of the ions and random collisions between the small particles and the ions. In a corona charging process, both diffusion and field charging occur for all particles, but as mentioned, field charging predominates for large particles and diffusion charging for small ones. In the intermediate range, both processes contribute significantly. In the absence of an electric field and where unipolar ions are present, the charging is only by the diffusion process. When bipolar ions are present, there will be charge neutralization.

If a particle is exposed to an ion concentration N_0 (ions/m^3), it will acquire in time t charge $q(t)$ given by

$$q(t) = \frac{4\pi\epsilon_0 rkT}{e} \ln\left(\frac{rN_0e^2ut}{4\epsilon_0 kT} + 1\right) \tag{69}$$

where r is the particle radius, k is Boltzmann's constant, T is the absolute temperature in kelvin, e is the electronic charge, and u is the mean thermal speed of ions (approximately 240 m/s). If the ions have more than one electric charge, e should be replaced by n_1, the ionic charge. Diffusion charging will continue until the electric field due to the surface charge of the particle exceeds the ionization potential of the gas.

Diffusion charging is extensively used for submicron particles. For example, in an electrical mobility analyzer, the ultrafine particles are charged with unipolar ions with single electronic charge and then analyzed according to their electrical mobility Z. Size classification of ultrafine particles is possible using a mobility analyzer.

Charge Neutralization

A major industrial application of diffusion charging is the neutralization of electrostatic charge on computer chips using bipolar ions of high concentration. Bipolar ions are produced using a corona discharge device driven by an ac voltage, usually 5 kV at a frequency of 60 Hz (4). Both positive and negative corona discharges are generated by using wire–cylinder electrode geometry. The positive and negative ions discharge the electrostatic charge on insulating or semiconducting surfaces where electrostatic charge neutralization is necessary. This type of ionizer is extensively used in semiconductor industries.

Another method of generating bipolar ions uses radioactive sources such as krypton-85 (^{85}Kr) and polonium-210 (^{210}Po). Radioactive sources generate bipolar ions, which can neutralize charged particles or surfaces. An advantage of radioactive sources is that no high voltage is necessary and hence they can be used where electrostatic sparks would be a serious hazard. However, the management of radioactive sources

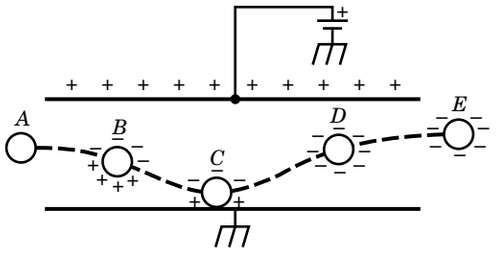

Figure 7. Induction charging of a spherical conducting particle that enters the electric field between two parallel plates and bounces off the grounded electrode with a net negative charge.

must be carried out according to the strict health safety regulations that apply to nuclear radiation.

Induction Charging

Induction charging is illustrated in Fig. 7. A spherical conducting particle that enters an electric field between two parallel plates experiences induction charging. At position *A* the particle's surface charge is uniformly zero. At *B*, negative charges are induced in areas close to the top positive plate, and the induced positive charges are repelled furthest from the positive plate. Once the ball touches the grounded plate at point *C*, the free positive charge leaks to the ground, leaving the bound induced negative charges. At positions *D* and *E*, the spherical conductor retains its excess negative charge. At position *E*, the excess negative charges are distributed uniformly across the surface in the field-free region.

In most cases the particles or droplets are charged with a polarity opposite to that of the induced charging electrode. However, induction charging with the same polarity is also possible, as shown in Figs. 8 and 9. Induction charging of a conducting liquid droplet is shown schematically in Fig. 10.

Induction charging requires that the surface or volume conductivity of the material be high enough for charge leakage to occur before separation of the object from the electrode (5). The time constant for the leakage of charge can be estimated from the charge relaxation time $\tau = \epsilon_0 \epsilon_r \rho$. Since $\epsilon_0 = 8.854 \times 10^{-12}$ F/m, the resistivity ρ should be less than 10^{10} $\Omega \cdot$ m for induction charging. For water, $\epsilon_r = 80$, and for the charging time to be 0.1 ms or less (6),

$$\rho = \frac{10^{-4}\,\text{s}}{8.854 \times 10^{-12} \times 80}\,\Omega \cdot \text{m} = 1.4 \times 10^{11}\,\Omega \cdot \text{m} \qquad (70)$$

Particles with higher resistivity will charge, but it will take longer. In the case of an ideal insulator, there is no free charge. However, in an electric field, the randomly oriented molecular dipoles become partly aligned in an external electric field according to the polarizability of the dielectric medium, but the net charge remains the same as before the application of the field. Induction charging is not applicable to the dry powder coating process, since the resistivity of the powder is generally too high. However, induction charging is routinely used in liquid-based spray painting.

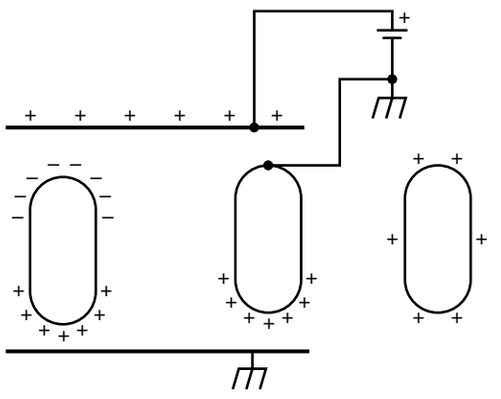

Figure 8. Induction charging of a metal fiber where the bound charges were neutralized, leaving charges of same polarity of the fiber.

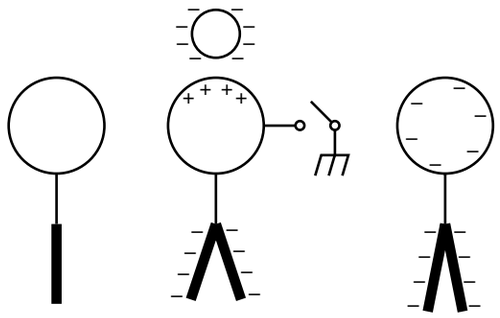

Figure 9. At the left is shown a discharged gold-leaf electroscope. In the middle a charged sphere is brought near and induction charging occurs. Bound charges are at the top of the electroscope, and free charges are on the leaves at the bottom. Grounding the sphere using a switch neutralizes the positive charge. If the grounding is disconnected and the charged sphere is moved far away, the entire electroscope becomes negatively charged.

Dielectrophoresis

An insulating particle placed in a uniform electric field experiences no electric force. However, in a nonuniform field, the

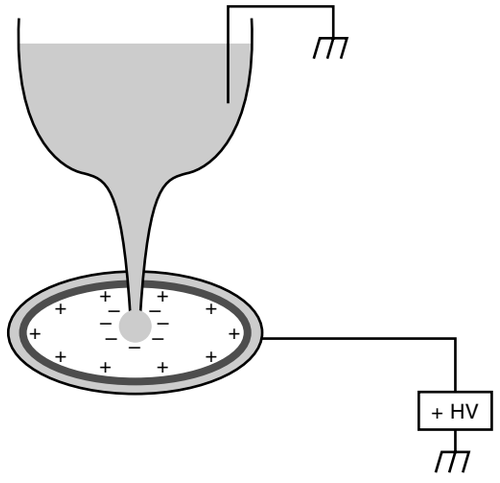

Figure 10. Induction charging of a conducting liquid. As the droplet leaves the nozzle, it carries charge with a polarity opposite to that of the ring electrode.

particle will polarize and move in the direction of the convergence of the electric field. This phenomenon is known as dielectrophoresis.

Triboelectric Charging

Tribocharging occurs through two mechanisms: (1) contact charging and (2) friction charging. In both cases, the mechanical processes that produce the charging of materials are: (a) sliding, (b) rolling or milling, (c) impact, (d) vibration of the surface at contact, (e) separation of solid–solid, solid–liquid, and liquid–liquid surfaces, and (f) deformation, leading to charge distribution at stress points. The amount of triboelectric charge exchanged between two contacting surfaces depends upon their relative speed and on the pressure between them. As the pressure increases, the area or the number of contact points increases. The surface charge density achieved by this process can be very high, up to 2×10^{13} e/m^2. At the maximum surface charge density the average distance between two charged atoms is only about 10 interatomic distances. Surfaces reaching the saturation charge level, however, contain no more than 8 to 10 electronic charges per million surface atoms.

Contact Charging. Contact charging between two surfaces does not require relative motion between them. The two surfaces are brought into physical contact. During this contact, charges move from one surface to the other.

There is a wealth of literature available on the contact charging process, but the experimental results are often contradictory and sometimes confusing. Two models that are most commonly used to explain contact charging are (1) electron transfer, and (2) ion transfer. Although material transfer has been considered by some investigators, its role in contact charging has not been fully established. In general, the transfer of electrons or ions can be explained by the surface-state theory. Several researchers, notably Schein (6), Hays (7), Lowel and Rose-Innes (8), and Cross et al. (3), have reviewed the electrostatic charging models in the light of their own work and that of other researchers such as Chowdry and Westgate (9), Harper (10), Krupp (11), Duke and Fabish (12), and Schein and Cranch (13).

Metal–Metal Contact Charging. When two metals of different work functions, ϕ_A and ϕ_B, are in contact, electrons tunnel from one surface to the other. The potential difference at the point of contact can be written as (6),

$$V_C = \frac{\phi_B - \phi_A}{e} \tag{71}$$

and the charge exchanged by tunneling between the two contacting surfaces can be expressed as

$$Q = C_{AB} V_C \tag{72}$$

where V_C is the contact potential and C_{AB} is the capacitance between the surfaces.

When the two metals are separated from each other, reverse flow of electrons takes place by tunneling. The tunneling stops when distance between the two surfaces exceeds 1 nm. Thus we have

$$Q = C_0 \frac{\phi_B - \phi_A}{e} \tag{73}$$

where $C_0 = C_{AB}$ at $d = 1$ nm.

The charge exchange is very rapid in metals; therefore, upon separation, the two surfaces are practically neutral. For metal–insulator or insulator–insulator contacts, there are residual charges upon separation.

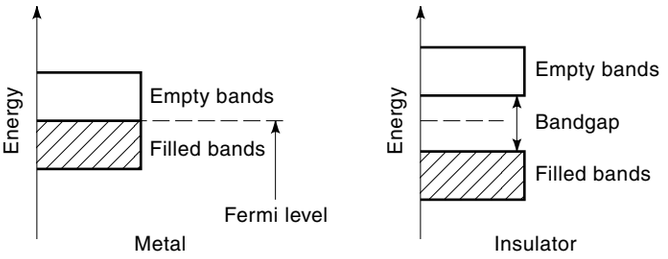

Figure 11. In a metal, the Fermi energy level lies between empty and fully occupied bands at 0 K. For an insulator, the conduction band is empty and the valence band is full with a large bandgap. However, the impurity atoms on the surface and the quantum-mechanical discontinuities of the surface wave function provide surface energy states that are partially full.

Metal–Insulator Contact. An ideal insulator has filled energy bands and an empty conduction band as shown in Fig. 11. At ordinary temperatures, there will be a few electrons in the conduction band and a few holes in the filled band, but the numbers of mobile electrons and holes are low. However, energy levels at the surface of the insulator are different from those of the bulk state due to surface discontinuities and imperfections. If we assume an equivalent work function ϕ_I for an insulator, we can write

$$Q = C_{MI} \frac{\phi_M - \phi_I}{e} \tag{74}$$

where C_{MI} is the capacitance between the metal and insulator surfaces. If we vary ϕ_M, that is, if we measure the exchange of charge Q between the insulator and different metals of Fermi levels ϕ_{M1}, ϕ_{M2}, . . ., and then plot Q versus ϕ_M, the intercept will indicate the value of ϕ_I when $Q = 0$. For metals, the work function ϕ_M can be plotted against a standard metal like gold. A linear relationship is expected. However, for many insulators linear relationships are not observed (6).

Fabish et al.'s (6) experiments showed that for contacts between an insulator and a metal, the insulator's surface gains a specific charge after a sufficient number of contacts. The charge is independent of previous charge levels of the insulator. The researchers explained the tribocharging of the insulator using the following model. The insulator has a range of localized energy levels (molecular-ion states), with a spread of 0 to 5 eV, caused by molecular vibration; furthermore, the charge exchange can occur only within a narrow window of the energy levels close to the metal's Fermi level ϕ_M.

An important property of contact charging is how these electronic energy states are filled. For an insulator, the sur-

face energy states are often partly filled. Schein (6) estimates that 10^{12} to 10^{15} energy states per square meter per electron volt may be involved in explaining some of the experimental data reported in the literature.

The ion-exchange process involves transfer of counterions from the powder (toner) surface to the surface of another material (carrier) with which the powder comes into contact. In summary, the driving forces and controlling parameters involved in the electrostatic contact charging process are:

1. The nature of the charge carrier (electrons or ions)
2. The difference in work function
3. Tunneling mechanisms
4. The energy states involved (surface or bulk, extrinsic or intrinsic)
5. The surface state densities
6. The type of contact, contact area, and friction involved
7. Particle–particle charging

In order to understand the charge transfer, it is necessary to understand the electronic surface energy structure of the materials.

Energy Bands. In an isolated atom, each electron has a quantum of energy. The defined orbits around the nucleus of an atom are considered as discrete energy levels. These levels are either *occupied* or *unoccupied* by electrons. When atoms are brought together to form a solid, there is considerable interaction between the different atoms. The electrons at the inner shells (or core bands) affect each other only slightly, whereas the electrons at the outer shells interact with each other more intensely, resulting in the widening of the energy levels from a discrete line structure into energy bands. The energy level that corresponds to the excited states of the outer electrons is called the conduction band. According to quantum mechanics, each band can only contain a fixed number of electrons. When all the energy levels are filled, it is called a filled band (Fig. 11).

A material can conduct electricity if outer electrons lie in an energy band that is partially empty. If the band is full, there are two electrons for every possible energy level in the band. No electron can increase its energy, and therefore electrons cannot be accelerated by the application of electric fields. For an electron to accelerate (gain energy), it must be able to find available space in the energy band. When the valence band is full, the material is an insulator.

The energy bands for metals and insulators are shown in Fig. 12. At temperatures above absolute zero (0 K), some of the electrons will gain energy and move to the conduction band, leaving empty energy levels or "holes" within the valence band. The number of mobile electrons and holes in an insulator is generally very small, and the resistivity is very high, on the order of $10^{14}\ \Omega \cdot \mathrm{m}$ or higher. A *crystalline insulator* has a large forbidden energy gap, up to 12 eV. A much higher temperature is required to move electrons to the conduction band from the valence band. A *semiconductor* is also an insulator at a low temperature. Its forbidden energy gap is on the order of 1 eV. At room temperature, there are sufficient numbers of electrons in the conduction band. A semiconductor or an insulator may contain impurity atoms. The impurity atoms can give rise to additional energy levels, either in terms of additional electrons in the conduction band (n-type) or holes in the filled valence band (p-type). These charge carriers permit the conduction of current (3).

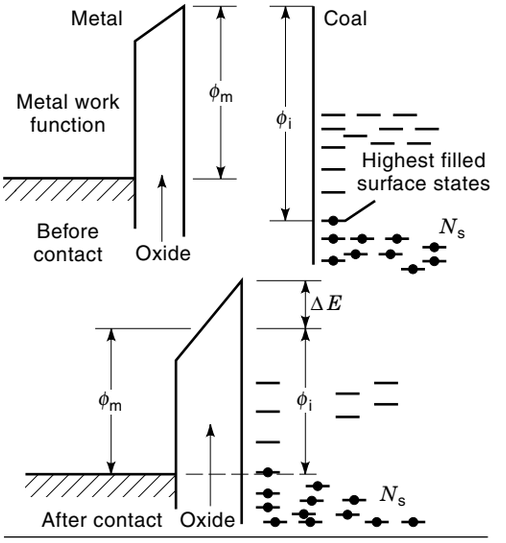

Figure 12. Contact charging of coal against a metal surface.

In some materials it is also possible to move electrons from the valence to the conduction band by irradiating the insulator surface with visible light or ultraviolet radiation. These materials are called *photoconductors.* For example, organic photoconductors, used in electrophotography, can store surface charges under dark conditions and are used to store latent images by appropriate surface illumination. Some insulators (for example, glasses and some conducting polymers) have *ions* that are relatively loosely bound to the main structure and can move in an electric field.

Charge control agents (CCAs) are added to improve charging characteristics of a powder (6). These are added either on the powder (e.g. toner) surface or to the bulk powder. Examples of surface charge control agents are (1) fumed silica (carbosil) and (2) kyner, a highly fluorinated polymeric material (polyvinylidene fluoride, manufactured by Pennwalt, or Saran F 220, manufactured by Dow Chemical). Bulk charge control agents are blended into the polymer. Among positive CCAs, bulk agents are (1) amino salts and (2) quaternary ammonium salts. In either case, large hydrocarbon chains with counterions, which can be halogens, fluoroborates, sulfates, or sulfanates, are used so that mobile counterions are transferred from one surface to the other. These materials are similar to antistatic agents, which are widely used to remove static charges. The antistatic agents are hygroscopic, and the moisture absorption at the surface promotes ionic conduction of charge. Among negative CCAs, the bulk agents are metal complex dyes.

Electrostatic Charging of Polymers

Polymer particles under dry conditions and at a low relative humidity are insulators with resistivity approximately $10^{14}\ \Omega \cdot \mathrm{m}$. For insulators that are partly amorphous, the lattice structure is disordered and there are localized energy levels within the bandgap of the insulator, due both to the discontinuities in the normal structure of the material at the surface,

and to the presence of impurity atoms. Both structural discontinuities and the impurity atoms at the surface contribute to the intrinsic and extrinsic surface states.

Theoretically, the number of surface states can be equal to the number of surface atoms; however, because of the maximum charge in a given environment, the actual density of the surface states active in a charge transfer process is much lower, generally in the range of 1 to 10 surface states per million surface atoms. Since there are approximately 2×10^{19} atoms/m^2, the surface state density generally ranges from 10^{12} m$^{-2} \cdot$ eV^{-1} to 10^{15} m$^{-2} \cdot$ eV^{-1}. It follows that surface impurity levels of few parts per million can significantly alter the nature of surfaces states and therefore the polarity and magnitude of electrostatic charge that an insulator surface can acquire. Since no real surface can be clean unless it is under an ultrahigh vacuum, physisorption and chemisorption of contaminants by surface atoms influences the electronic surface structure of the insulator and the resulting electrostatic charging. Often, these uncontrolled surface properties often lead to unpredictable electrostatic charging.

Electron Transfer

In metal–insulator contact charge exchange, different metals deplete or fill the surface states of the insulator, depending upon the position of the *surface work function* of the insulator with respect to the Fermi level of the metal. There are a number of external factors involved in contact charging under ambient conditions. First, there is a metal oxide layer, which is always present when a metal is exposed to air. Second, the particles are also often coated with an oxide layer and other contaminants. The contact charge exchange density σ on the insulator can be expressed as (7)

$$\sigma = eN_s(\phi_i + \Delta E - \phi_m)\left(1 + \frac{e^2 N_s d}{\epsilon}\right)^{-1} \tag{75}$$

where ϕ_i is the surface work function of the insulator, ϕ_m is the Fermi level of the metal surface, ΔE is the energy gap created by the oxide layer, N_s is the surface state density per unit area per unit energy (eV), e is the electronic charge, d is the thickness of the oxide layer, and ϵ is the permittivity of the oxide layer. In the limit of low surface state density, $e^2 N_s d/\epsilon \ll 1$, and if we include a factor f to represent the fraction of geometric area that makes intimate contact, then Eq. (75) can be approximated as

$$\sigma = f\epsilon N_s(\phi_i + \Delta E - \phi_m) \tag{76}$$

In the limit of high surface state density, $e^2 N_s d/\epsilon \gg 1$, Eq. (75) simplifies to

$$\sigma = f\epsilon \frac{\phi_i + \Delta E - \phi_m}{ed} \tag{77}$$

The above expressions show that contact charging depends upon the surface oxidation and on the density of the surface states. The physical meaning of ϕ_i, the surface work function of an insulator, is not clearly established, nor is it known how surface states are distributed within the forbidden energy gap of the insulator.

Equations (76) and (77) show the two limiting cases that are often considered in the surface state theory of charge transfer: (1) low surface density and (2) high surface density. In the first case, the number of charges exchanged between the metal and the insulator is equal to the number of surface states, and is low enough that the electric field between the metal and insulator does not cause a significant shift in the insulator energy levels. In contrast, in the limit of high surface density, as the large number of surface states get filled, there is a strong electric field between the metal and insulator, raising the energy levels of the insulator surface states, which limits further charge transfer (3). Until very recently, the low-density limit was considered to be the case for most metal–insulator charging processes; however, Schein (6) has shown that, particularly for toners, the charge transfer data can be better explained assuming the high-surface-density limit where the interfacial electric field controls the charge transfer process.

Ion Transfer

In the ion transfer model, u_i represents a chemical potential. Ion transfer depends upon the difference in affinities of two contacting surfaces for specific ions. Harper's model, as discussed by Schein (6), estimates the surface charge density after contact as

$$\sigma_s = N_i \exp\left(-\frac{u_1 - u_2}{kT}\right) \tag{78}$$

where N_i is the surface density of ions, and u_1 and u_2 are the potential energies of the two surfaces or their affinities for the ions in the ions transfer process, respectively.

Real surfaces are always covered with adsorbed layers, which are frequently ionic in nature, or contain a charged double layer. An adsorbed water layer 10 μm thick will be a substantial potential barrier to the transfer of electrons. However, ion exchange can take place across the contacting double layer. Direct observation of ion transfer in contact charging between a metal and a polymer has been reported in the literature (6).

FRICTION CHARGING

In addition to the contact process, temperature differences between the contact points are considered to be an additional factor in tribocharging. The exchange of charge (q) can be related to the force (F) of contact as (3)

$$q \propto F^a \tag{79}$$

where a is a factor (0.3 to 1) that depends upon the type of contact.

Gidaspow et al. (14) considered the impact velocity V and computed the charge exchange following a model developed by Chang and Soo:

$$Q = K_1 K_2 |V|^{0.6} d_p^2 \rho_p^{0.8} (\phi_i - \phi_m) \frac{N_i N_m}{N_i + N_m} \tag{80}$$

where K_1 and K_2 are constants depending upon the mechanical properties of the materials (Poisson's ratio and Young's modulus) and upon the ratio of the rebound speed to the incoming speed, d_p and ρ_p are the particle diameter and density,

V is the velocity, ϕ_i and ϕ_m are the work functions of the insulator and metal, respectively, and N_i and N_m are the corresponding surface state densities.

ELECTROSTATIC PRECIPITATORS

The electrostatic precipitator was the first major industrial application of electrostatics. The principles of electrostatic precipitators were demonstrated in the late 1800s. In 1907, Professor F. G. Cottrell used an electrostatic precipitator to collect acid mist emitted by a sulfuric acid manufacturing plant. Cottrell's research resulted in the application of electrostatic precipitators to the control of air pollution and the recovery of materials from copper, lead, and zinc smelters, and to the removal of fly ash (the particulate ash product that results from burning pulverized coal in power plants, blast furnaces, and aluminum reduction plants). Electrostatic precipitators have also been used in residential applications for cleaning air. Electrostatic precipitation involves two steps: (1) the charging of the particles by corona discharge, and (2) precipitation of the charged particles by the application of an electric field. An air-handling device is used to pass the gas through the precipitator.

There are two types of electrostatic precipitators. In the smaller ones, the particles are charged in the first stage and are deposited by use of a precipitating electrostatic field in the second stage. In large industrial electrostatic precipitators (1,2), both charging and deposition are performed by the same set of electrodes. The corona generation process was discussed in the preceding section. One of the major advantages of the electrostatic precipitator is that unlike mechanical gas-cleaning devices, where enormous energy is spent to treat the entire gas to remove the particles, the energy to remove the particles from the flow gas in a precipitator is primarily spent on the particles themselves. As a result, the energy consumed by electrostatic precipitators is much less than by mechanical gas-cleaning devices such as cyclones and bag filters. The pressure drop across a precipitator is much lower than that across cyclones and filter bags for the same gas flow rate and particulate collection efficiency.

There are two basic geometries utilized in electrostatic precipitators: (1) wire–cylinder geometry, where a high voltage is applied to a wire coaxially located within a large cylinder (Fig. 5) through which particle-laden gas passes, and (2) parallel plate electrode geometry (Fig. 13), where a series of wires are positioned symmetrically across large parallel grounded plates. The wires are connected to a high-voltage supply, usually negative. In both cases, the corona process starts at the wire, to which a high negative voltage is applied to generate negative corona. Negative ions, mainly O_2^- ions, travel from the high-voltage wire electrode to the cylinder or to the parallel plates. During their passage along the field line, the ions deposit on the particles. In most cases, the particles reach their saturation charge during their transit through the precipitator, and because of the electrostatic field and image forces, particles deposit on the surfaces of the collector electrodes. Thereupon, the charge decay process begins. The rate of decay of the charge depends on the resistivity of the particles. As the particles approach a collector electrode, the image forces between the charged particles and the grounded electrode dominate, particularly when the distance between the particles and electrode surface is only a few millimeters. Depending on the charge of the particles and their resistivity, particles will adhere to the collection plate because of the image forces. If a particle's charge decays fast, the force of adhesion decreases also and the particle can slide off of the collecting wall, thereby keeping the collection electrode's surface clean. However, if the particles are resistive or sticky in nature, they will adhere to the collector's surface until they are cleaned off mechanically. This is done by *rapping,* in which mechanical forces dislodge the deposited particles from the collector wall. Liquid drops, such as sulfuric acid drops, lose charge when they are collected on the electrode. The resulting liquid film drains off, and can be collected and stored.

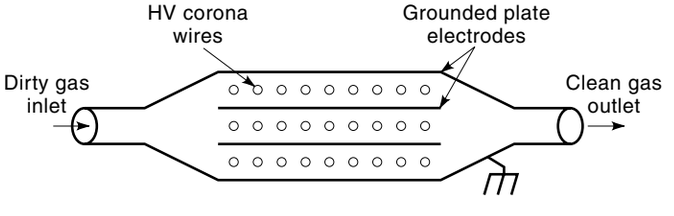

Figure 13. Wire–plate electrode geometry used in an industrial precipitator.

Conducting solid particles will lose their charge rapidly but can recharge to the opposite polarity by induction as discussed in the preceding section. Such oppositely charged particles may travel back toward the discharge electrode, where they will become recharged to the polarity of the corona discharge. As a result, the conducting particle can bounce back and forth. Therefore the electrostatic precipitator technique is not suitable for highly conducting particles, with the exception of liquid droplets.

Charging of the particles or droplets in an electrostatic precipitator takes place by two mechanisms: (1) field charging, where the ions follow electric field lines and land on the particle surface, where charging continues until saturation, and (2) diffusion charging, where the ions collect on the particle surface because of their thermal motion. Most particles larger than 2.0 μm in diameter are primarily charged by field charging, whereas particles smaller than 0.5 μm are charged more efficiently by diffusion charging. In an electrostatic precipitator, both mechanisms operate simultaneously, and for particles 0.5 μm to 2.0 μm in diameter, both processes contribute significantly. During the charging process, the particles must reside for a sufficiently long time to acquire electrostatic charge close to their saturation level so that the charged particles can be removed efficiently from the gas stream by the electric field.

The electrical migration velocity of the charged particle in an electrostatic precipitator, under an idealized condition, is given by (4)

$$W = \frac{qEC_C}{3\pi\mu d_P} \tag{81}$$

where W is the migration velocity of particles of diameter d_P, η is the viscosity of a gas, E is the electric field, and C_C is the Cunningham slip correction factor. The above equation describes the particle motion in an idealized condition where the gas flow is considered laminar. However, in most precipita-

tors the gas flow is turbulent. The particles arrive near the boundary layer of the collecting wall by the turbulent motion of the fluid flow. When charged particles are close to the wall, electrostatic attraction forces become effective for their deposition. Using this turbulent model, Deutsch derived the collection efficiency (CE) as follows:

$$\mathrm{CE} = 1 - \exp(-W_E S_C / Q_G) \tag{82}$$

where W_E is the effective migration velocity (m/s), S_C is the total collection area (m^2), and Q_G is the gas flow rate (m^3/s). The effective migration velocity is based upon the turbulent flow model. Deutsch's equation does not include nonlinear effects. Modification of this equation is therefore necessary, because several nonlinear factors, including corona quenching, variation of space charge, back corona, and a high-resistivity dust layer, are present in an actual precipitator.

The major components of an electrostatic precipitator are:

1. *High-Voltage Supplies.* Power supplies usually range up to −100 kV. The current capacity depends upon the total surface area of the precipitator. A typical ion current concentration on the collector plates is 10^{-4} A · m^{-2}. From the collector plate design, the current capacity for each power supply is determined.
2. *Corona Charging Sections.* In most industrial electrostatic precipitators, charging and precipitation are performed by the same electrodes. For residential application, a two-stage precipitator is used, where the dust particles are charged in the charging section and are then precipitated by using parallel plate electrodes. In most industrial precipitators, negative high voltage is used, primarily for two reasons: (1) negative corona is more stable, and (2) one can operate the negative corona at a much higher voltage than a positive corona. Negative corona produces more ozone than positive corona, and since ozone is a health hazard, negative corona is not used for residential air cleaning. For residential applications, electrostatic precipitators use positive corona.
3. *Collector Electrodes.* Depending upon the geometry, both parallel plates and cylindrical pipes are used for particle collectors. Coal-fired power plants employ large parallel plate precipitators.
4. *Rapping Device.* Used for mechanically agitating the collecting electrodes to dislodge the dust collected on the surface of the electrodes.
5. *Gas-Handling Device.* Used to move the dust-laden gas into the precipitator, and move the clean gas from the precipitator to a discharge stack or to another device for further cleaning.

INK JET PRINTING

There are two basic ink jet printing (4) mechanisms: (1) drop-on-demand and (2) continuous. In the drop-on-demand process, each drop is produced on demand (i.e. when needed on the target surface) by the application of pulsed energy—thermal or piezoelectric. In the continuous process, a high-pressure jet is used to produce a fine stream of liquid. The nozzle, usually with diameter 35 μm, is vibrated at a frequency greater than 100 kHz to synchronize the jet breakup into droplets of uniform size. A cylindrical electrode is used to apply an electric field for induction charging of the droplets. Using a set of deflection electrodes, the drops are diverted at high speed to the desired spots on the target for printing. When the droplets are not needed, the power supplies to both the charging and deflection electrode systems are turned off and the uncharged and undeflected ink drops are sent to a gutter, from where the ink is recirculated back to the reservoir after filtration.

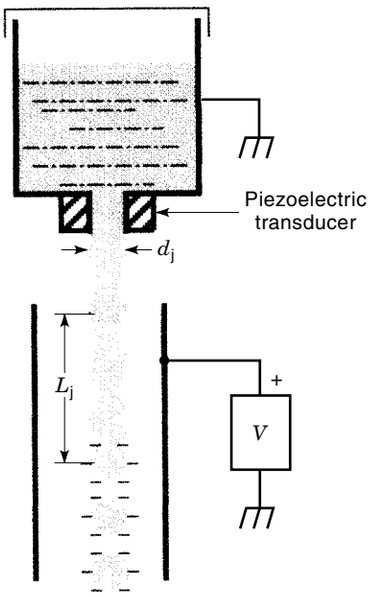

Figure 14. Induction charging of conductive droplets produced by ultrasonic excitation.

Continuous ink jet systems are widely used for industrial printing such as the printing of packaging materials and mass mailing materials. The ink jet nozzle is operated at about 200 kPa pressure and is vibrated at a frequency of 100 kHz or higher. Figure 14 shows the droplet generation and induction charging process. There are a few critical parameters involved. When a jet of length λ and diameter d_j breaks into droplets of diameter d_d, we can write, by equating the fluid volumes (4,5),

$$\frac{\pi d_j^2 \lambda}{4} = \frac{\pi d_a^3}{6} \tag{83}$$

λ is also called the surface wavelength. Krein and Robinson give the following relationships (4):

$$\lambda = 4.5 d_j \tag{84}$$

$$d_d = 1.89 d_j \tag{85}$$

If each drop is to be formed in a time period t_d, which is typically 10 μs, the jet velocity U_j can be written as

$$U_j = \lambda / t_d = 4.5 d_j / t_d \tag{86}$$

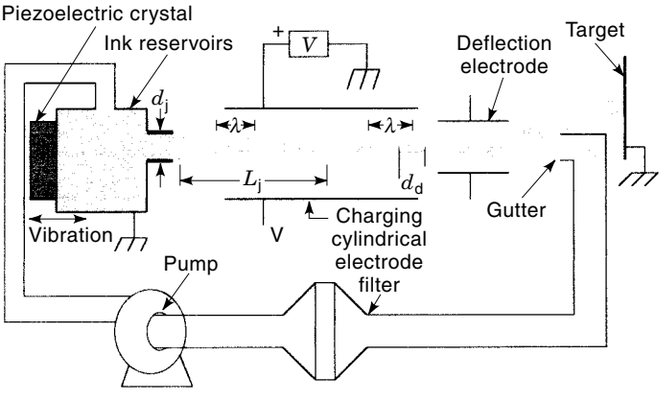

Figure 15. A continuous ink jet generator used for printing.

For a droplet diameter not to exceed 100 μm, d_j is chosen to be about 35 μm; therefore, U_j is 15.75 m/s. A static pressure as high as 470 kPa is often used to force ink through a jet of diameter 38 μm. An experimental arrangement of an ink jet printer is shown in Fig. 15.

During the formation of the droplets, small satellite droplets are also formed. Usually, it is desired to operate the jet without forming satellites, which is possible by adjusting t_d and λ/d_d. Approximately 300 V is applied to the cylindrical electrode to charge droplets to near saturation with a charge-to-mass ratio higher than 2 μC/g.

The droplet charge q_d can be written as

$$q_d = \frac{4.75\pi\epsilon_0 d_d}{\ln(D_e/d_j)} \tag{87}$$

where d_d is the droplet diameter, D_e is the diameter of the cylindrical electrode used for applying electric field, and d_j is the diameter of the ink jet.

A piezoelectric crystal is used to vibrate the nozzle in the direction of the ink flow (Fig. 15). The vibration frequency f depends upon the wavelength λ and the capillary wave velocity V_c along the jet surface:

$$V_c = f\lambda \tag{88}$$

where

$$V_c = (4\sigma/\rho d_j)^{1/2} \tag{89}$$

where σ is the surface tension, ρ is the density of the liquid, and d_j is the jet diameter. V_c is about 2 m/s. The excitation frequency f breaks the capillary into f drops per second. In a typical continuous ink jet operation, more than 100,000 drops, of approximately 100 μm diameter, are produced per second.

POWDER COATING PROCESS

Process Description

Powder coating (3,15) is a multidisciplinary field comprising powder technology and electrostatic engineering. It involves: (1) polymer science, (2) powder manufacturing, (3) fluidization and transport of powder, (4) particle charging and dispersion, (5) electrostatic spraying and coating, (6) curing and melt rheology, and (7) process modeling and optimization.

In an electrostatic coating process, the powder is first fluidized so that it can be pneumatically conveyed, at a controlled mass flow rate, from a reservoir to the spray gun, where it is electrostatically charged and sprayed toward the grounded workpiece to be painted (Fig. 16). The aerodynamic forces of the atomization air transport the charged particles from the spray gun to the vicinity of the workpiece. Near the surface of the workpiece, the electrostatic image force between the charged particles and the grounded metal surface dominates, causing the particles to deposit on the surface. Coating is performed in a powder coating booth. Workpieces to be coated are moved to the booth using a conveyor belt, and are then moved to an oven for curing the powder layer (thereby forming a film) on the surface.

The four forces acting between the charged particles and the conducting substrate are: (1) the electrostatic image force of attraction between charged particles and the grounded workpiece, (2) the coulombic repulsive force between particles arriving at the substrate and the deposited particles charged with the same polarity, (3) van der Waals forces, and (4) force due to external electric fields. These attractive and repulsive forces compete with each other, and the resultant forces hold the particles onto the workpiece until the coating is cured in the oven.

Advantages of Powder Coating

Electrostatic powder coating is an environmentally safe, economically competitive, high-quality painting process for metals and plastics. The oversprayed powder can be recycled back into the coating process to achieve better than 95% material utilization. This high-efficiency application contrasts dramatically with solvent-based coating, which creates serious environmental and energy-related problems. The volatile organic compounds (VOCs) used in most solvent-based coating processes are hazardous to human health and therefore require pollution control measures to incinerate the vapor and the overspray. Special care is needed in the manufacturing, storage, transportation, and application of these hazardous substances. The oversprayed, solvent-based products cannot be reused, resulting in considerable material loss.

The powder coating process has a large industrial base in the United States, with a growth rate of 10%/yr or more, depending upon the specific industry. For example, as early as 1994, American powder coating sales were up by 15% over the same sales period in 1993. All market categories in powder coating rose in 1994, e.g., architectural finishing was up

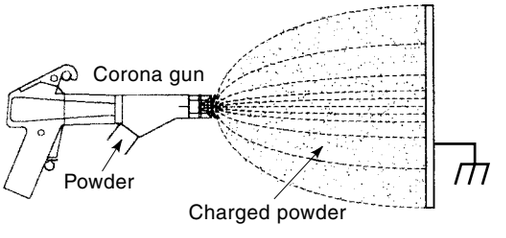

Figure 16. A schematic showing a powder coating setup with a corona gun and a flat grounded metal plate. A high voltage up to −100 kV is applied to the corona gun.

57%; lawn and garden, 26%; appliances, 17%; automotive, 20%; and general metal finishing, 9%.

Technological advances in powder coating may open large market opportunities. Automotive clear coats in particular may drive US industrial growth rates in powder coating up to 10% or more annually through this decade. The big three US auto manufacturers—GM, Ford, and Chrysler—have formed a low-emission paint consortium to advance powder coating. Other automotive companies, including BMW, have begun adding top clear-coat using a powder spray process.

Film Appearance

The greatest challenge faced by the powder coating industry is to produce a surface finish comparable to, or even better than, the solvent-based process. Current powder coating technology produces an *orange-peel* texture, which is unacceptable to auto manufacturers for exterior surface coats. The solvent-based painting process produces a superior glossy appearance with better weatherability. Therefore, powder coating in auto manufacturing is limited to the interior surfaces and top clearcoats of the automobile. The three primary advantages of a dry process—environmental safety, high transfer efficiency, and cost-effectiveness in the painting of the exterior surface of the automobiles—will not be realized unless better appearance of the surface finish, chip resistance, and weathering characteristics are achieved. For these purposes it will be necessary to optimize the electrostatic properties, melt rheology, and surface chemistry of powders. The formulation, particle size distribution, charging, transport, and deposition of powders on the target surface need to be controlled to minimize the orange-peel texture and to produce a glossy finish that will withstand outdoor exposure in Florida (Florida Exposure Test) for 20 years or more.

Process Optimization and Reduction of Back Corona

Optimization of material formulation and electrostatic and thermal properties may eventually make the process superior to solvent-based coating in all respects. Currently, both tribocharging and corona charging methods are used in the electrostatic spray painting process. However, corona charging is most widely used in the powder coating industry. The corona discharge process is discussed in the section "Charging of Materials and Transport of Charged Particles" above. The corona discharge results in a reproducible charging of powder; however, only a portion of the ion current is utilized in charging. Since the discharge produces large amounts of ions, the charged particles and the remaining ions deposit on the substrates along with the powder layer. This ionic current charges the powder layer and causes dielectric breakdown in it, resulting in back corona. Back corona produces an orange-peel textured surface, unacceptable in many applications. Surface textures can be controlled in the corona discharge method if the electrical resistivity can be optimized by appropriate powder formulation or by spraying powder at a high relative humidity, around 60%. Currently no method is readily applicable to control the volume resistivity of powders for powder coating applications.

When the gun voltage is increased or the gun-to-workpiece distance d is decreased, there is an increase of ion current [see Eq. 52(b)], which may increase back corona and reduce particle deposition efficiency even further. When the back corona process was not well understood, powder coating process operators often would increase the gun voltage to improve transfer efficiency, only to find that the outcome was opposite to what was anticipated. Currently, manufacturers of powder coating guns use a feedback control system to maintain a constant corona current by varying the high voltage applied to the gun so as to minimize back corona. Back corona can be observed under dark conditions as a diffuse glow on the powder surface. An image intensifier tube can be used to map back corona on a powder layer.

Equation 52(a) shows how the ion current I increases with the voltage V applied to the gun. Since the charge-to-mass ratio of the powder and the initial transfer efficiency increase with V, it is necessary to adjust V to an optimum point where ion current is low for good appearance while overall transfer efficiency is high.

Back corona can also occur when there is no ion current but the electric field within the powder layer has exceeded the breakdown voltage. If q_v is the charge per unit volume of the powder layer and t is its thickness, we can write from Gauss's law

$$EA = \frac{q_v A t}{\epsilon_0 \epsilon_r} \tag{90}$$

where A and t are the area and thickness of the powder layer, E is the electric field across the powder layer, and ϵ_r is the dielectric constant of the powder layer. At the breakdown point, the field can be written as

$$E_b = \frac{q_v t}{\epsilon_0 \epsilon_r} \tag{91}$$

The interstitial air in the porous powder layer will break down at $E_b \approx 3 \times 10^6$ V/m. E_b will be much higher for a solid film (see Table 5). If we consider the breakdown voltage of the powder layer is as high as 10^7 V/m, then maximum charge per unit volume, for $t = 100$ μm and $\epsilon_r = 2$, is

$$q_v = 1.17\,\mathrm{C/m^3} \tag{92}$$

If the density of the powder layer is approximately 1000 kg/m^3,

$$(q/m)_{max} = \begin{cases} 1.17\,\mu\mathrm{C/g} & \text{for } E_b = 10^7 \text{ V/m (dielectric)} \\ 0.39\,\mu\mathrm{C/g} & \text{for } E_b = 3 \times 10^6 \text{ V/m (air)} \end{cases} \tag{93}$$

The above equation shows that back corona may occur in a powder layer of 100 μm thickness when the charge-to-mass ratio of the powder exceeds 1.77 μC/g. In most applications, charge-to-mass ratio varies from 0.5 μC/g to 1.0 μC/g, but the breakdown electric field can be lower than 10^7 V/m. A mini-

Table 5. Dielectric Breakdown Field for Different Media

Dielectric Medium	Breakdown Electric Field (V/m)
Air	3×10^6
Polystyrene	2.4×10^7
Teflon	1×10^7
Barium titanate	5×10^6
Mylar	1.5×10^8

mum value of q/m of the powder is needed for good adhesion. One experimental study indicates that q/m should be larger than 0.2 μC/g (3).

Tribocharging produces no ion current, but presently it is not reliable for consistent charging of the powder. Both fundamental and experimental research studies are needed to overcome some of the engineering problems. Current understanding of contact and tribocharging of nonconducting particles needs to progress to a level where electrostatic charging processes can be controlled in a quantitative manner. While the major engineering problems have been solved for toner charging in the electrophotographic process through extensive experimental studies, tribocharging is still considered unreliable and unpredictable for powder coating applications. For example, a typical powder coating system requires simultaneous operation of 16 powder coating guns, each delivering 60 g to 100 g of powder per minute. Once the inner walls of triboguns are coated with powder, the charging efficiency decreases. The triboguns to be used in the powder coating process must be able to operate continuously in a reliable manner.

ELECTROPHOTOGRAPHY: COPYING MACHINES AND LASER PRINTERS

About the same time electrostatic precipitators became widely used in industry for removing particulate materials from gas, a new application of electrostatics was emerging—electrophotography. Electrophotography is used in office copiers and laser printers, by far the most successful industrial application of all electrostatic engineering processes. It accounts for approximately $50 billion in annual sales in the global economy. In 1937, Chester Carlson invented this electrostatic copying process, which merged two branches of physics, electrostatics and photoconductivity. For more details on electrophotography, see ELECTROPHOTOGRAPHY.

Electrophotography (6,15,16) is similar to optical photography, where a silver halide film is used to first store a latent optical image on its surface. The film is then developed to print the image on photographic paper. The electrophotographic process uses a photoconducting surface, where electrostatic charges are deposited uniformly for storing a latent image, as shown in Fig. 17. A characteristic of photoconductors is that in the dark they are insulators, so that surface charge can be stored for a long time. However, when light is incident on the photoconducting surface, the charge decays rapidly. Therefore, a charged photoconducting surface can be used to store an optical image either by writing on it with a laser beam (as in laser printers) or by exposing the surface to an optical image of a document (as in copying machines). The basic difference between these two processes is that in laser writing it is the discharged area that retains the information, and thus toners need to be deposited on the discharged area. This is known as discharged area development (DAD). In the copying process, information is usually stored in black on a white background, like this printed page. An optical image of a document on the photoconducting surface will therefore discharge the background area (white), leaving the charged area (black) with the information. In this case, a charged area development (CAD) is used, where toners are deposited on the charged surfaces. These processes are illustrated in Fig. 17.

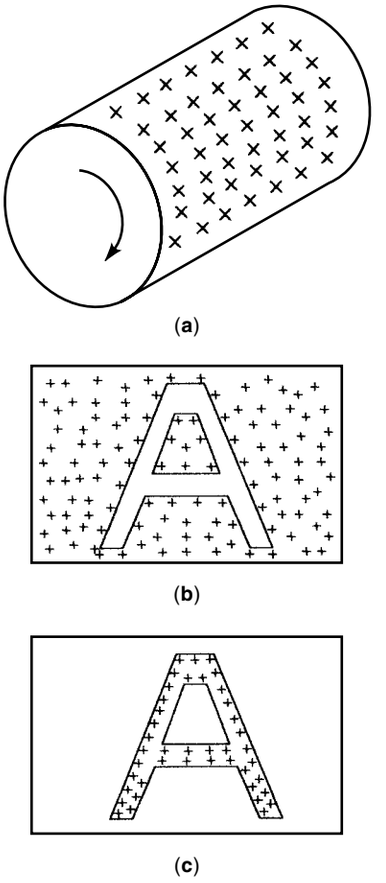

Figure 17. (a) A corona-charged photoconducting drum. (b) A latent image of the letter "A" formed by a laser beam scanner on a positively charged photoconducting film (laser printer). (c) A latent image of the letter "A" formed by the copying process.

There are six basic steps in the electrophotographic process, as shown in Fig. 18, that are applicable to both copying machines and laser printers:

1. *Corona Charging of the Photoconducting Surface.* The photoconducting surface, kept under dark conditions, is corona-charged to produce a uniform charge distribution on it (see Fig. 17).
2. *Exposure of the Photoconducting Surface.* The charged surface is exposed to a scanning laser beam or to an optical image of the document. An electrostatic latent image is stored when information to be printed is written on the photoconducting surface, or reflected light from a document illuminated by white light is incident on it.
3. *Development of the Latent Image.* Electrostatically charged pigmented toner particles, with a size distribution from 6 μm to 8 μm in diameter, develop the latent image on the surface of the photoconductor.
4. *Transfer of the Developed Image.* The image developed by the deposition of toner is then transferred from the photoconducting surface to an appropriate medium, such as paper or transparency, for use. A corona device is used to spray charged ions on the back of the page to

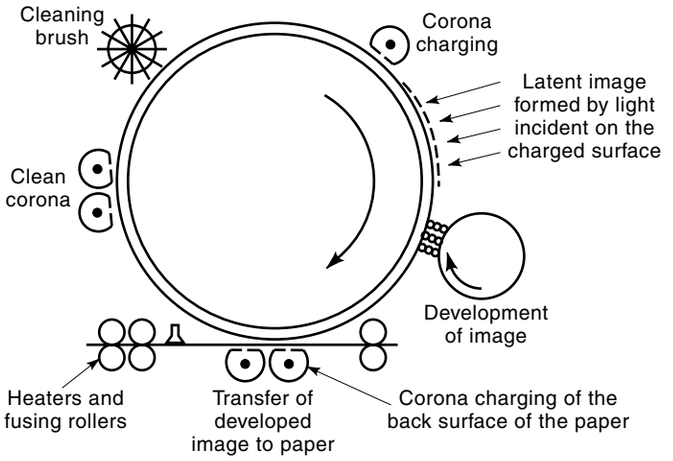

Figure 18. An electrophotographic process showing six steps to printing or copying: (1) charging, (2) latent-image formation, (3) image development by charged toner, (4) transfer of image to paper, (5) fusing of image on paper, and (6) cleaning.

attract toners of opposite charge from the photoconductor to the paper.

5. *Fusing of the Toner Particles on the Medium.* The toners are permanently fixed on the surface of the paper by applying heat and pressure.
6. *Cleaning of the Photoconducting Drum and Preparation for the Next Cycle.* The cleaning process requires an ac corona discharge, so that charged particles still adhering to the photoconducting drum can be discharged and then dislodged by a mechanical cleaning brush. Similarly, after fusing of the toner on the surface of the medium, the high electrostatic charge on the media must also be removed to eliminate electrostatic cling and sparking.

Corona and tribocharging processes are involved in electrophotography, and exact control of the charging process is essential for ensuring excellent performance of copying machines and laser printers. It took more than 40 years of research to achieve the current state of the art in copying machines, laser printers, and ink jet printers. These printing processes are often collectively called nonimpact printing.

Toner Charging and Development

Toners are polymer particles 2 μm to 20 μm in diameter. The polymers are polystyrenes, polyacrylics, polymethacrylites, or other polymer materials, blended with about 10% by weight carbon black or other pigments. A host of other materials are also used to obtain various desired properties. These additives include charge control agents to attain appropriate charge, flow agents to ensure appropriate powder flow of the toner materials during development, and fusing agents to obtain the desired surface finish after fusing of the toners on the medium's surface. Toners are always charged triboelectrically in one of two ways: (1) a two-component development process where toner particles are charged against carrier particles (magnetic particles, coated with an appropriate polymer layer, in the size range 50 μm to 200 μm in diameter) to provide electrostatic charge of controlled magnitude and desired polarity to the toners; or (2) a one-component development process where toner particles are blended with magnetic materials that are triboelectrically charged against the surface of the development roller, and then against a doctor blade. The flow of toner particles from the reserve to the photoconducting drum is produced by the movement of the roller film over a bank of stationary magnets, which attract the magnetic toner to the surface of the roller. No carrier powder is used in this case.

In the two-component development process, the toner particles are attracted to the latent image on the photoconducting surface by the electrostatic attractive forces while the carrier particles are held on the development roller by magnetic forces. In the one-component development process, toner particles are made magnetic in order to facilitate the flow of toner by the development roller to the photoconducting drum.

Extensive theoretical and experimental studies have been performed on the toner charging and development processes. In medium- and high-speed copiers and laser printers, two-component development is used, whereas one-component toners are generally used in low-speed personal copiers. It is difficult to accurately analyze the process of toner development because of the complexity of the electric field distributions and the dynamic nature of the process, which changes the field as a function of the development time. In spite of this difficulty, a number of theoretical and empirical models have been successfully developed and implemented commercially through numerous patents and publications.

ELECTROSTATIC SEPARATION

Basic Mechanisms

Triboelectric separation of coal from minerals, quartz from feldspar, phosphate rock from silica sand, rubber from fabric, zircon from rutile, phosphorus and silica from iron ore, and diamond from gangue has been successfully demonstrated in laboratory experiments, pilot plant studies, and, in some cases, commercial plants (3,14,17–19). The process is very attractive from both energy usage and economic points of view. Electrostatic separation is achieved by exploiting differences in the resistivities of the materials or their tribocharging characteristics. In the first process, a rotating-drum separator is generally used. Particles are fed from a vibrating hopper to the surface of a conducting drum, which rotates at an optimum rate. First the particles are charged in a corona charging zone. As the particles move further from the charging zone, the conducting particles (e.g., iron ore) lose their charge rapidly and fall off the drum. The insulating particles (e.g., sand) retain their charge and therefore remain attached to the drum surface until they are removed with a mechanical brush. In the second process, materials are separated by their tribocharging characteristics. The tribocharging process utilized in dry coal cleaning is an example of charge separation, and is discussed below.

Electrostatic Beneficiation Process for Coal Cleaning

With the electrostatic cleaning method (14), coal is first pulverized into a fine powder of particles 5 μm to 750 μm in diameter. The powder is then electrostatically charged by impact against a metal surface such as copper. On contact with

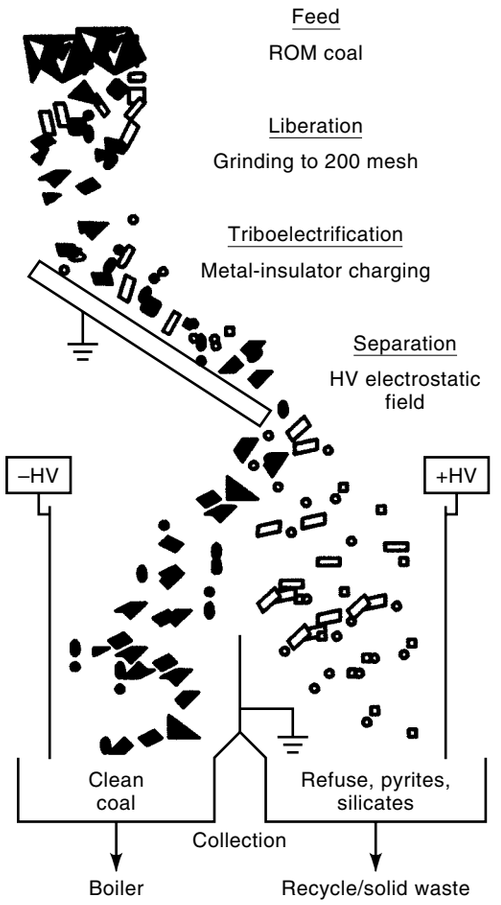

Figure 19. Electrostatic physical cleaning of coal.

the copper, the organic coal particles become positively charged and the pyrites and inorganic mineral particles become negatively charged. If this tribocharged powder is passed through an electrostatic separator consisting of two high-voltage conducting plates, the material separates on the basis of the polarity of the electrostatic charge. The experimental arrangement is shown in Fig. 19. The organic coal particles are attracted toward the negative plate, whereas the pyrites and mineral particles are attracted toward the positive plate. The primary energy expended in electrostatic separation is for grinding the coal particles to a size that liberates most of the mineral inclusions from the organic coal matrix. Coal is pulverized down to −200 mesh for conventional boilers in power plants. Wet cleaning also requires liberation of the mineral inclusion. Therefore, the separation process in electrostatic dry cleaning does not require any finer grinding, and it uses less energy than the wet cleaning process, since no dewatering and drying are necessary. Furthermore, since dewatering is not required, there is no risk of stream pollution.

Previous studies on electrostatic beneficiation of coal have shown significant progress, and it is of commercial interest in many countries, as shown in Table 6. However, the process has not been implemented on a commercial scale. Many fundamental aspects of the tribocharging process involved in semiconducting and insulating materials are not well understood (6). Many factors influencing the efficiency of beneficiation also remain poorly understood. This is due in large part to the great complexity of coals, which have been subjected to biomorphic and geomorphic changes over very long time periods. Coal is a heterogeneous rock consisting of discrete maceral and mineral components, something like a fruitcake (19). Coals from diverse localities have widely differing compositions and structures and hence variable charging properties.

Electrostatic Charging of Coal and Minerals

Coal particles under dry conditions and low relative humidity are insulators with resistivity approximately $10^{14}\ \Omega \cdot m$, whereas pyrite particles are semiconductors with a resistivity of $10^{7}\ \Omega \cdot m$. The resistivity of coal particles will depend greatly upon their moisture and ash content, and thus different types of coal will have different resistivity. For insulators that are partly amorphous, the lattice structure is disordered and there are localized energy levels within the bandgap, due both to the discontinuities in the normal structure of the material at the surface and to the presence of impurity atoms. The surface of coal has abundant impurities. Discontinuities and the impurity atoms at the surface contribute to the intrinsic and extrinsic surface states. Figure 12 shows the contact charging process between coal and copper.

Inculet et al. (20) observed that vitrinite macerals have a tendency to be positively charged, while fusinite and semifusinite charge negatively. Experimental data obtained by them in coal fractions separated in an electrostatic process indicate that while a major fraction of the vitrinite charged positively, a significant portion charged negatively. Most of the pyrites, however, charged negatively. More recently Kwetkus (21) studied coal samples from France, Great Britain, and the United States and found that in most cases the coal particles charged negatively. However, when run-of-mine (ROM) coal was processed by flotation to reduce the ash content, the organic coal particles charged positively against copper. Kwetkus also showed that (1) the maximum negative charge acquired by coal particles decreased monotonically with increasing relative humidity, (2) the maximum charge acquired by mineral particles such as calcite, quartz, and pyrite were orders of magnitude lower than that acquired by the coal particles, and (3) while some of the mineral particles acquired significantly greater charge at elevated temperatures, other mineral particles did not when the temperature was varied from 20° to 80°C.

In metal–insulator contact charge exchange, different metals deplete or fill the surface states of the insulator, depending upon the position of the *surface work function* of the insulator with respect to the Fermi level of the metal. In the coal beneficiation process, ROM coal particles are charged against copper. Inculet measured the work functions as follows: maceral coal particles, 3.93 eV; mineral pyrites, 5.40 eV; copper, 4.38 eV. If these values hold for a given coal beneficiation process, the maceral coal will be charged positive and pyrite negative. However, as we have noted earlier, experimental data on the charge distribution of coal particles show wide variation in polarity and magnitude.

Effect of Particle Concentration

In a commercial-scale operation, the particle concentration inside the separator will be high. Increasing particle concentra-

Table 6. Milestones in Electrostatic Separation of Coal from Minerals

Year	Country	Description
1914	United States	Schniewend—patent on triboelectric separation of coal
1940	Germany	Pilot plant studies—reduction of ash (15% to 1.5%)
1976	United States	Singewald—pilot plant operation with 5 ton/h feed rate
1977	Canada	Inculet—electrostatic loop separator
1983	Japan	Masuda—cyclone triboelectric separator
1984	Italy	Ciccu—rotating-wheel impact tribocharger
1987	United States	Gidaspow and Wasan—Electrofluidized bed and electrostatic sieve conveyors
1987	United States	Advanced energy dynamics (AED)—drum-type separator
1990	United States	Link and Finseth (DOE/PETC)—static copper charger and separator dynamics
1992	China	Chen—drum separator
1995	United States	Stencel (AER,KY)—workshop on dry separation technology

tion has two attendant problems: (1) there will be a significant space charge between the two electrodes, which will interfere with the separation, and (2) the frequency of interparticle collisions will be high, causing coagulation of positive and negative particles and thus decreasing the separation efficiency. It is anticipated that most of the collisions will be related to the turbulent shear stress, which increases with the flow Reynolds number. The number of particle collisions per second can be estimated as (14)

$$n = 0.27C\frac{du}{dy}\frac{d_{\mathrm{p}}^{1/2}}{\lambda^{1/2}} \tag{94}$$

where C is the concentration of particles, u is the velocity of the particle stream, λ is the mean free path of the particles (the average distance between collisions), and du/dy is the velocity gradient in a turbulent air flow. Since the number of collisions will increase with residence time, it will be necessary to reduce the residence time and therefore increase the velocity. However, since turbulence will increase the collision frequency, the separator must be designed to have minimum flow fluctuations.

Particle Size Effect

Inherent in any physical cleaning process is the assumption that the materials to be separated can be physically liberated from each other. For the electrostatic beneficiation of coal, the mineral particles must be liberated from the coal matrix during crushing and grinding. Liberation of pyrites has been studied by Irdi et al. (22) and by Dumm and Hogg (23) using froth flotation and density separation, respectively. The effect of particle size distribution on the efficiency of beneficiation has been studied in some cases.

ELECTROSTATIC HAZARD CONTROL: ELECTROSTATIC DISCHARGE BY DUST EXPLOSION

Electrostatic discharge (ESD) (4) may cause explosion in an atmosphere where a combustible powder or vapor is dispersed in air. Since many polymeric powders are highly resistive and can store charge easily, it is necessary to take appropriate precautions where there is a significant ESD ignition risk.

There are three requirements for a dust explosion: (1) fuel such as a combustible powder, (2) an oxidizing agent, such as oxygen gas, and (3) an ignition source such as an electrostatic discharge or a lighted match. Many airborne dusts are flammable in a limited range of particle concentration (usually 80 g/m^3 to 2000 g/m^3) depending upon the particle size distribution and the composition of the powder. As the effective particle size decreases, specific surface area increases and combustible dust becomes more ignitable. Similarly, there is a minimum oxygen concentration requirement for ignition. Also, the energy of the ignition source must be equal to or greater than the minimum ignition energy (MIE) for explosion.

The MIE required to ignite powder at a given concentration increases with the mean particle diameter d_{50} (μm). For example, for polyethylene and aluminum flakes, the MIE varies from 10 mJ to 500 mJ as d_{50} increases from 0.1 μm to 10,000 μm according to the approximate empirical relationship.

$$\mathrm{MIE} = \phi(d^3) \tag{95}$$

The probability of explosion, P_{e}, can be expressed as

$$P_{\mathrm{e}} = P_{\mathrm{f}}P_{\mathrm{i}} \tag{96}$$

where P_{f} is the probability of existence of a flammable powder–air mixture and P_{i} is the probability of the simultaneous presence of an ignition source with MIE.

For example, during the filling of a tank with combustible powder or a liquid, charge can accumulate until a condition is reached when the stored electrostatic energy is suddenly released by a spark exceeding the MIE, causing explosion.

Triboelectric charge generation in the pneumatic transport of powder can be as high as 100 μC/kg. A large volume of stored powder with such high specific charge per unit mass presents ignition hazards. When the resistivity of the powder is higher than $10^{12}\ \Omega \cdot \mathrm{m}$, the charge relaxation time constant is sufficiently long to pose ignition hazards due to accumulation of charge. The relative humidity plays a critical role. When it is greater than 60% the charge decays quickly and the risk of ignition decreases significantly.

If there is an ungrounded conductor that can accumulate charge caused by the collection of charged particles, the voltage V on the conductor can be estimated from its capacitance, since $V = Q/C$. Capacitance discharge accounts for most electrostatic ignitions. For ignition, the spark energy U_{e} must exceed the MIE, that is,

$$U_{\mathrm{e}} = \tfrac{1}{2}CV^2 \geq \mathrm{MIE} \tag{97}$$

The maximum sparking potential voltage V_{max} must satisfy

$$V_{max} \leq 350\,V \tag{98}$$

In general, an upper limit of 100 V is used to supply a margin of safety. As a rule of thumb, when V exceeds 100 V, there is a chance of electrostatic spark.

It is important to note that corona discharge is, in general, not a cause of electrostatic ignition. Spark discharge is much more energetic than corona discharge. Sparking represents a negative resistance condition causing a high flow of current for a very short duration.

The propagating brush discharge is perhaps one of the most common sources of ESD ignition. When an insulating layer on a conductive backing accumulates a high surface charge density and comes close to a conducting object, it is possible to have an ESD with spark energy much greater than the MIE. A typical brush discharge condition is shown in Fig. 20. The maximum surface charge that can accumulate on the insulating layer can be much higher than the maximum surface charge density for an isolated body. The insulating layer on a conductive backing acts like a distributed capacitor by storing energy. When the charged insulating layer comes close to a conducting object, an electrostatic charge may run along the surface. Therefore, it is not recommended to use plastic lining against a metal pipe for transport of powder. The capacitive energy per unit area can be written as

$$U_e = \tfrac{1}{2} C_L V_L^2 \tag{99}$$

where

C_L = capacitance per unit area = $\epsilon_r \epsilon_0 / t$
$V_L = \sigma_s / C_L$
σ_s = surface charge per unit area

Ignition is possible when U_e becomes greater than 1.2 mJ/cm^2 in a brush discharge. When the surface charge is greater than 25 nC/cm^2, the thickness t of the insulating layer should be much larger than 1 mm. A propagating brush discharge can have energy release in excess of 1 J.

In *silos,* most dust explosions are caused by *Maurer discharge* during the filling. Particles of diameter larger than a few hundred micrometers do not cause ESD ignition hazard, but fines, which are almost always present, can result in a flammable atmosphere. During the filling operation, larger particles acquire charge because of their higher velocity and cause brush discharge.

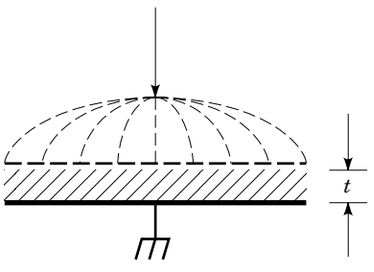

Figure 20. An insulating film or powder layer accumulating charge can be discharged to a grounded object with propagating brush discharge, causing ignition. When the surface charge density exceeds 3×10^{-6} μC/m^2, there is a probability of brush discharge (1–3 mJ). A propagating brush discharge (100 J) occurs when the surface charge density exceeds 2×10^{-4} C/m^2 on a thin insulating layer over a grounded conducting surface.

Pneumatic transport of flammable powder can also be hazardous. Since the charge-to-mass ratio depends upon the velocity of the powder, it is possible to avoid ESD ignition risk by using metal tubes of large diameter to reduce friction during filling. The danger is small when the powder transported is not stored. For example, in a powder coating process, insulated rubber hose is used for flexibility, but since the powder is deposited on a metal surface and is not stored in a large volume, the ESD hazard is minimal. However, the metal workpiece receiving the charged powder must be well grounded to minimize ESD ignition hazards. For resin powder, the MIE is approximately 5 mJ: therefore, the spark energy needs to be maintained below 0.5 mJ for powders in powder coating applications.

Static Charges on a Human Body

Electrostatic charge on a human body can also cause ignition hazard. People walking on an insulating floor wearing insulated shoes and nylon clothing, or touching electrostatically charged objects, can acquire a potential up to 15 kV. A typical capacitance of a human body is 200 pF. When a person with a high charge touches a grounded conductor, the spark energy can be as high as 10 mJ, which can exceed the MIE in some cases.

The human reaction to ESD depends upon the energy of the spark. Below 1 mJ, the ESD is often not detectable. At 10 mJ, there is a pricking sensation; at 100 mJ, the electric shock is unpleasant; above 1 J it is painful; and at about 100 J spasm or even death may occur.

ESD Hazard Control

The following safety procedures are generally recommended.

1. Ground all conductive parts and equipment.
2. Use passive methods of discharge:
   a. Decrease the velocity.
   b. Increase the relative humidity.
   c. Use antistatic materials.
   d. Use thin rods or static bars (1 mm to 3 mm diameter) inside the storage silos. Ground the rods well to promote corona discharge or brush discharge in discharging the powder store.
   e. Neutralize charges by using a pointed metal rod connected to the ground and placed inside a pipe with the tip projecting into the powder flow stream, which may initiate corona discharge and generate ions for neutralization.
3. Decrease the resistivity when possible. There is a direct relationship between resistivity threshold and MIE. For example, if the MIE is 10 mJ, the resistivity should not exceed 10^9 $\Omega \cdot$ m. Increasing the RH to 60% or higher increases the surface conductivity of many polymer materials.

All conductors must be well grounded. To avoid sparking, the recommended safe upper limit of potential difference is 100 V. Most sensitive devices should be grounded with resistance no greater than 10^6 Ω. A grounding resistance also decreases the energy of the spark.

Active Charge Neutralizers. Bipolar ionizers can be used to neutralize static electricity. In this case, the charge is not discharged to ground but is neutralized by the coulombic attraction between the charged objects and mobile ions. Bipolar ionizers are extensively used in the semiconductor industry as static eliminators. These ionizers are commercially available. They employ ac corona at a frequency 50 Hz or 60 Hz. Pulsed positive and negative square waves are also used. In many cases, air is passed through a grounded nozzle where a HV electrode is positioned coaxially with an applied voltage between 3 kV and 5 kV ac. Pulsed dc ionizers are often preferable so that the pulse length and frequency can be adjusted to minimize recombination of bipolar ions.

Neutralization Using a Radioactive Source. In some cases where conventional ionization process cannot be used, particularly in areas where electrical devices may create additional hazards, radioactive sources are used for air ionization. Polonium-210, an alpha source, is commonly used to produce strong ionization in a small confined area. Krypton-85, a beta emitter, is also used to neutralize charged particles at a low concentration.

Induction Ionizers. Induction ionizers are commonly used to neutralize areas of high static charge generation. Typically, these passive neutralizers consist of sharp, grounded needlepoints placed opposite charged surface. The induced charge at the needlepoint causes corona discharge, thereby producing ions to neutralize charges. For neutralization, the charge induced must be high enough to initiate corona discharge.

Static Bars. Static bars are arrays of bars used to inject ions either by corona discharge or by using nuclear radiation. Such static bars are often used in areas of high static charge generation.

BIBLIOGRAPHY

1. H. J. White, *Industrial Electrostatic Precipitation,* Oxford: Pergamon, 1963. See also K. R. Parker (ed.), *Applied Electrostatics Precipitation,* Blackie Academic and Professional, 1997.
2. S. Oglesby, Jr. and G. Nichols, *Electrostatic Precipitation,* New York: Marcel Dekker, 1978.
3. J. A. Cross, R. Morrow, and G. Haddad, An analysis of the current in a point to plan corona discharge and the effect of a porous insulating layer on the plane, *J. Appl. Photonic Eng.,* **7**: 121–125, 1986.
4. J. Chang, in A. J. Kelly and J. M. Crowley (eds.), *Handbook for Electrostatic Processes,* New York: Marcel Dekker, 1995, pp. 733–747.
5. A. G. Bailey, *Electrostatic Spraying of Liquids,* New York: Wiley, 1988.
6. L. B. Schein, *Electrophotography and Development Physics,* New York: Springer-Verlag, 1988.
7. D. A. Hays, Contact electrification between metals and polymers: Effect of surface oxidation, *Proc. Int. Conf. Modern Electrostatics,* 1989, pp. 327–330.
8. J. Lowell and A. C. Rose-Innes, Contact electrification, *Adv. Phys.,* **29**: 947–1023, 1980.
9. T. J. Lewis, The movement of electrical charge along polymer surfaces, in D. T. Clark and W. J. Feast (eds.), *Polymer Surfaces,* New York: Wiley-Interscience, 1978, Chap. 4.
10. W. R. Harper, *Contact and Frictional Electrification,* Oxford: Clarendon, 1967.
11. H. Krupp, Physical models of static electrification of solids, in *Static Electrification,* Inst. Phys. Conf. Ser. 11, 1971, pp. 1–17.
12. C. B. Duke and T. J. Fabish, Charge induced relaxation in polymers, *Phys. Rev. Lett.,* **37**, 1075–1078, 1976.
13. A. R. Blythe, *Electrostatic Properties of Polymers,* Cambridge, UK: Cambridge Univ. Press, 1978.
14. D. Gidaspow et al., Separation of pyrites from Illinois coals using electrofluidized beds and electrostatic sieve conveyors, in Y. P. Chugh and R. D. Caudle (eds.), *Processing and Utilization of High Sulfur Coals II,* New York: Elsevier Science, 1987.
15. J. F. Hughes, *Electrostatic Powder Coating,* New York: Research Studies Press and Wiley, 1985.
16. E. M. Williams, *The Physics and Technology of Xerographic Processes,* New York: Wiley, 1984.
17. O. C. Ralston, *Electrostatic Separation of Mixed Granular Solids,* Amsterdam: Elsevier, 1961.
18. D. Whitlock, Advanced physical fine coal cleaning, Advanced Energy Dynamics Report, DOE Contract #DE-AC22-85PC81211, December 1987.
19. M. K. Mazumder, D. A. Lindquist, and K. B. Tennal, Electrostatic beneficiation of coal, *Inst. Phys. Conf. Ser. 143,* 1996, p. 385.
20. I. I. Inculet, M. A. Bergougnou, and J. D. Brown, Electrostatic beneficiation of coal, in Y. A. Liu (ed.), *Physical Cleaning of Coal—Present and Developing Methods,* New York: Marcel Dekker, 1982, pp. 87–131.
21. B. A. Kwetkus, Contact electrification of coal and minerals, *J. Electrostatics,* **32**: 271–276, 1994.
22. G. A. Irdi, S. W. Minnigh, and R. C. Rohar, Pyrite particle size distribution and pyritic sulfur reduction in crushed coals: A preliminary report, *Particulate Sci. and Technol.,* **8**: 123–136.
23. T. F. Dumm and R. Hogg, Distribution of sulfur and ash in ultrafine coal, in Y. P. Chugh and R. D. Caudle (eds.), *Processing and Utilization of High Sulfur Coals II,* New York: Elsevier Science, 1987.

Reading List

J. Chang, A. J. Kelly, and J. M. Crowley (eds.), *Handbook for Electrostatic Processes,* New York: Marcel Dekker, 1995.

J. A. Cross, *Electrostatics: Principles, Problems and Applications,* Bristol: Adam Hilger, 1987.

J. M. Crowley, *Fundamentals of Applied Electrostatics,* Melbourne, FL: Krieger, 1991.

H. Haus and J. R. Melcher, *Electromagnetic Fields and Energy,* Englewood Cliffs, NJ: Prentice-Hall, 1989.

J. D. Jackson, *Classical Electrodynamics,* New York: Wiley, 1962.

A. D. Moore, *Electrostatics and Its Applications,* New York: Wiley, 1973.

H. A. Paul, *Dielectrophoresis,* Cambridge, UK: Cambridge Univ. Press, 1978.

MALAY K. MAZUMDER
University of Arkansas at Little Rock